Use of Fibroin/Hyaluronic Acid Matrices as a Drug Reservoir in Iontophoretic Transdermal Delivery

By

Emre KUDUĞ

A Dissertation Submitted to the
Graduate School in partial Fulfillment of the
Requirement for the Degree of

MASTER OF SCIENCE

Department: Chemical Engineering
Major: Chemical Engineering

İzmir Institute of Technology
İzmir, Turkey

February, 2004

ACKNOWLEDGMENTS

I would like to acknowledge the guidance and support of my thesis advisor Asst. Prof. Ayşegül Batıgün and co-advisor Asst. Prof. Oğuz Bayraktar. I am grateful to Prof. Devrim Balköse for providing the peristaltic pump used in this study.

I would like to acknowledge the support of IYTE research fund (Project code AR-FON 017), Iomed, Inc. (Utah, USA) for donation of the iontophoresis power supply, and Bursa Institute for Silkworm Research for providing raw silk.

I would like to thank my colleague Özge Malay, my dearest friend Yelda Ergün and my dear friend Beyhan Cansever for their support and help in the experiments and also in the writing of this thesis.

ABSTRACT

Transdermal drug delivery is gaining importance due to the extensive research in genetics and resulting increase of protein and peptide based drugs in the market. In order to develop materials to be used in iontophoretic transdermal drug delivery systems, various forms of silk fibroin (SF) and blending agents as hyaluronic acid (HA) have been tested for their feasibility as a potential drug reservoir. For this purpose different forms of silk such as raw silk, degummed silk fibroin, insolubilized freeze-dried fibroin, membranes of fibroin in pure and blended with HA were investigated for their adsorption capacities of timolol maleate, which is used as the model drug. It was found that silk fibroin and derivatives have considerable adsorption capacities for timolol maleate with 0.35 mmol per gram, comparable with commercial membranes. The insolubilization of the membranes was required for drug loading and delivery in aqueous media. Membrane insolubility was achieved by post treatment, manipulation of drying conditions, and blending with different agents. Configurational changes of fibroin protein and interactions between silk fibroin and hyaluronic acid were investigated by Fourier transform infrared spectroscopy, scanning electron microscopy, and X-ray diffraction analyses. Insoluble fibroin glutaraldehyde membranes were produced. The obtained insoluble membranes were investigated for drug delivery performance in a custom-made diffusion cell under passive diffusion and iontophoretic conditions. It was demonstrated that the silk fibroin glutaraldehyde films could be successfully used for controlled drug delivery. It was found that current densities of 1.5 and 3 mA/cm^2 were suitable to accomplish controlled delivery of the drug in a pulsatile manner. The results of this study are expected to be useful in controlled transdermal delivery of positively charged drug molecules.

ÖZ

Genetik bilimindeki kapsamlı araştırmalar ve bunun sonucu olarak protein ve peptit içerikli ilaçların piyasadaki miktarının artmasıyla deri yoluyla ilaç iletimi önem kazanmaktadır. İyontoforetik deri yoluyla ilaç iletim sistemleri geliştirmek amacıyla ipek fibroininin çeşitli formlarının ve hyaluronik asit ile karıştırılmış fibroinin potansiyel ilaç deposu olarak kullanılabilirlikleri test edilmiştir. Bu amaçla ipeğin pek çok formunun, örneğin ham ipek, pişirilmiş ipek fibroini, dondurulup kurutularak çözünmeyen hale getirilmiş fibroin, saf ve hyaluronik asit ile karıştırılmış fibroin membranlarının model ilaç olarak kullanılan timolol maleat`ı adsorplama kapasiteleri incelenmiştir. İpek fibroin ve türevlerinin ticari membranlarla kıyaslanabilir ve kayda değer düzeyde timolol maleat adsorpsiyon kapasitelerine sahip oldukları saptanmıştır. Sulu ortamda ilaç yüklenmesi ve iletimi için membranların çözünmez olması gerekmektedir. Membranın çözünmezliği sonradan işleme metodları, kurutma koşullarının ayarlanması ve farklı kimyasallarla karıştırma suretiyle sağlanmıştır. Fibroin proteinin şekilsel değişiklikleri ve ipek fibroini ile hyaluronik asit arasındaki etkileşim Fourier transform kızılötesi spektroskopisi, taramalı elektron mikroskobu ve X-ışını kırınımı analizleriyle incelenmiştir. Çözünmeyen fibroin glutaraldehit membranları ve metanol ile işlenmiş fibroin membranları üretilmiştir. Elde edilen çözünmez membranların pasif difüzyon ve iyontoforetik koşullar altında ilaç iletim performansları özel yapım difüzyon hücresi kullanılarak incelenmiştir. İpek fibroin glutaraldehit ve metanol ile işlenmiş fibroin filmlerin kontrollü ilaç iletimi için başarıyla kullanılabileceği gösterilmiştir. İlacın darbeli tarzda kontrollü iletimi başarılmıştır.

TABLE OF CONTENTS

LIST OF FIGURES viii
LIST OF TABLES x
Chapter 1 INTRODUCTION 1
Chapter 2 TRANSDERMAL DRUG DELIVERY 3
2.1. Controlled Drug Delivery 3
2.2. Methods of Transdermal Delivery 4
2.2.1. Passive Diffusion 4
2.2.2. Phonophoresis 5
2.2.3. Electroporation 5
2.2.4. Iontophoresis 5
2.2.5. Selection of Electrodes 8
Chapter 3 DRUG RESERVOIR MATRIX: PREPARATION OF INSOLUBLE SILK MATRIX 9
3.1. Silk Fibroin 9
3.2. Methods of Silk Fibroin Matrix Preparation 13
3.3. Previous Studies with Silk Fibroin 17
3.3.1. SFGTA Blends 17
3.3.2. Freeze-Dried SF 18
3.3.3. SF Film with Glutaraldehyde 18
3.3.4. Other Studies with Silk Fibroin 19
3.4. Hyaluronic Acid 19
3.5. Previous Studies with Hyaluronic Acid 21
3.6. Insoluble Matrix Preparation 23
3.7. Preparation of Silk Fibroin/Hyaluronic Acid Solution 24
Chapter 4 LOADING AND DELIVERY OF MODEL DRUG TIMOLOL 25
Chapter 5 EXPERIMENTAL 28
5.1. Preparation of Silk Fibroin Solution by Ajisawa's Solution 28
5.2. Preparation of Drug Loading Reservoirs 30
5.2.1. Preparation of Different Forms of SF 32
5.2.2. Preparation of SF/HA Films 33
5.2.3. SF Film Crosslinked with Glutaraldehyde 33

5.2.4. Freeze-Dried SF 34
5.3. Characterization of the Membranes 34
5.3.1. Solubility Tests 35
5.3.2. Analysis Methods 35
5.4. Adsorption Experiments 35
5.5. Iontophoretic Experiments 36
Chapter 6 RESULTS 39
6.1. Characterization of the Membranes 39
6.1.1. Effect of Post Treatment on the Structure of Silk Fibroin 39
6.2. Formation of SF Film 44
6.2.1. SF/HA Films 44
6.3. Glutaraldehyde Cross-Linked SF Film 47
6.4. Adsorption Experiments 47
6.5. Diffusion Experiments 49
6.5.1. Passive Diffusion Experiments 50
6.5.2. Active Diffusion Experiments 51
CONCLUSIONS 61
REFERENCES 62
APPENDIX A A1
APPENDIX B A2
APPENDIX C A3
APPENDIX D A4

LIST OF FIGURES

Figure 2.1 Drug level in blood for traditional (a) and controlled (b) drug delivery 3
Figure 2.2 1. Iontophoretic delivery system 2. Electrode system applied to the skin surface. 6
Figure 3.1 a) Domestic silkworm building its cocoon b) Finished cocoon c) Reeled silk9
Figure 3.2 β pleated structure of silk fibroin a) Face view b) Side view.....11
Figure 3.3 Scheme for the molecular shape of SF molecules in solution and solid state for aqueous system.....13
Figure 3.4 Conformation change of SF in solid state by immersion in methanol (Green boxes represent long-range ordered crystallite) 14
Figure 3.5 The relation between conformation, quenching or casting temperature and (starting) concentration of silk fibroin, B. mori [37] 15
Figure 3.6 Chemical structure of hyaluronic acid [64] (arrow indicates carboxyl group) 20
Figure 3.7 Structure of HA in its native form [70] 21
Figure 3.8 Carboxyl-amino interaction in the chitosan-alginate polyelectrolyte complex 24
Figure 4.1 Structure of timolol maleate salt. 26
Figure 5.1 Preparation of silk fibroin solution.....29
Figure 5.2 Block diagram describing various forms of SF and SF/HA blends produced in this study. 31
Figure 5.3 Custom-made diffusion cell used for drug delivery experiments 37
Figure 5.4 Iontophoresis experiment set-up 38
Figure 6.1 SEM image of cross-section of a) Methanol treated SF (SFMT) membrane. Magnification: 12000x. b) Heat treated SF (SFHT) membrane. Magnification: 5000x.....40
Figure 6.2 a) SEM image of freeze-dried SF sponge. Magnification: 2000x. b) Magnification: 650x. c) After methanol treatment. Magnification: 2000x. d) First frozen then freeze-dried SF. Magnification: 250x. 41

Figure 6.3 X-Ray diffractograms of SF films treated in methanol a) for 3 minutes (SF-MT 3 min) b) for 6 minutes (SF-MT 6 min) c) for 10 minutes (SF-MT 10 min) d) Heat treated SF film dried at 45 ^{o}C. 42
Figure 6.4 Ft-Ir spectra of a) silk film and b) methanol treated silk film. 43
Figure 6.5 SEM image of cross-section of soluble membranes. Composition: 50% HA, 50% SF. Magnification: 10000x. b) Composition: 70% HA, 30% SF. Magnification: 6500x. 45
Figure 6.6 SEM image of cross-section of insoluble membranes. a) Composition: 15% HA, 85% SF. Magnification: 6500x. b) Composition: 10% HA, 90% SF. Magnification: 6500x. 45
Figure 6.7 X-Ray diffractograms of a) 10% HA insoluble film (smoothed). b) 15% HA insoluble film (smoothed). 46
Figure 6.8 Ft-Ir spectra of a) HA film b) 10% HA, 90% SF soluble film c) 10% HA, 90% SF insoluble film d) SF film 48
Figure 6.9 Results of adsorption experiment. Equilibrium concentrations. 49
Figure 6.10 Passive drug delivery for SFGTA drug loaded film. I=0. 50
Figure 6.11 a) Iontophoretic drug delivery for SFGTA drug loaded film. b) Current application course with I=1 mA. 52
Figure 6.12 a) Iontophoretic drug delivery for SFGTA drug loaded film. b) Current application course of two current applications of I=2 and 4 mA. 54
Figure 6.13 Iontophoretic drug delivery experiment for SFGTA membrane. Pulsed current application of I=4 mA a) Delivery of drug b) Current application course. .55
Figure 6.14 Iontophoretic drug delivery experiment for SFGTA membrane. Pulsed current application of I=2 mA a) Delivery of drug b) Current application course. .56
Figure 6.15 Iontophoretic drug delivery experiment for SFGTA membrane. Pulsed current application of I=1 mA a) Delivery of drug b) Current application course. .57
Figure 6.16 Iontophoretic drug delivery for SFGTA membranes pulsed current application values of 1, 2, and 4 mA. 58
Figure 6.17 X-Ray diffractogram of methanol treated (10 min) SF film after iontophoretic experiment. 59
Figure 6.18 X-ray diffractograms of SFGTA film a) Before iontophoresis b) After iontophoresis 60

LIST OF TABLES

Table 3.1 Amino-acid content, g/ 100 g fibroin 10
Table 3.2 Some of the related companies with HA or HA-derived products on the market 22
Table 6.1 Insoluble Samples 40
Table 6.2 Weight ratios of the two components in the polymer matrices. 44
Table 6.3 Dose applications and corresponding drug release for iontophoretic experiments 59

CHAPTER 1

INTRODUCTION

Controlled delivery of drugs is a vast research topic studied by many scientists and researchers throughout the world. In traditional drug delivery, concentration of the drug exhibit peaks, which may go beyond maximum desired level and waste the drug material or even, be toxic. The desired level is between the minimum efficient and maximum desired level [1].

The recent researches in genetics study suggest that more drugs based on proteins and peptides will be in the market in the near future [2]. Though these drugs will be more efficient than those of today's, and will be tailored to the specific needs of the patient, the only drug delivery route is the intravenous route for protein based drugs. This means the average patient will have to have several injections daily. Injection is not convenient since it produces a sudden peak in blood drug concentration, is accompanied by pain, brings infection risk, and does not fit the pace of life of the 21st century individual.

The aim of this study is to develop a drug loading reservoir from silk fibroin which could be used under passive and iontophoretic conditions. Chapter 2 covers the subject of transdermal delivery. In Chapter 3, preparation of soluble/ insoluble matrices, under different treatment conditions and blending agents as hyaluronic acid (HA), and glutaraldehyde (GTA) were explained. Chapter 4 reviews previous studies in transdermal delivery, iontophoresis and studies on timolol maleate adsorption and delivery. Procedures of SF matrix preparation, adsorption of TM and iontophoretic experiments are explained in Chapter 5. The results are given in Chapter 6.

Transdermal route is one of the routes of drug delivery to the body. Transdermal drug delivery offers significant potential for the non-invasive delivery of drugs. The skin provides a large, accessible surface area, in addition to avoiding the hepatic first-pass effect and chemical degradation in the hostile environment of the gastrointestinal tract [3]. Transdermal drug delivery systems employ a carrier that

supplies the therapeutic agent to the organism continuously at the desired level, while the human skin is practically built to protect the body from outer effects and foreign materials. To overcome this barrier, various chemical, physical and electrical methods have been developed to help drug molecules penetrate the skin. One of these methods is the iontophoretic method which incorporates a drug reservoir containing charged drug molecules, where the molecules are driven into the body by application of electrical current. The transdermal iontophoretic delivery is gaining popularity as a new and convenient method.

The positively charged silk fibroin, which has an isoelectric point around 4 is promising for controlled adsorption and desorption of positively charged drug molecules. It is known that silk fibroin derived from *Bombyx mori* cocoon is being developed and utilized for purposes besides traditional textile material. It is used as surgical sutures, food additives, and in cosmetics. Its superior properties like biocompatibility, high thermal-stability, and microbial resistance had it proposed for purposes such as wound protection, substrate for cell culture, enzyme immobilization, soft contact lenses with high oxygen permeability, and drug release agents [4]. Fibroin can be easily made up to into various forms [5], like film, membrane, gel, powder, and fiber [6]. In this research potential of silk fibroin as a drug reservoir was investigated. Films and fibers were subject to drug uptake experiments and membranes were tested for drug transport through them. Effect of current application on the diffusion rate and responsiveness of delivery to current is investigated.

CHAPTER 2

TRANSDERMAL DRUG DELIVERY

2.1. Controlled Drug Delivery

Oral administration of drugs may deactivate the drug molecules or have toxic effects. The concentration of the drug in the blood may exceed the maximum desired level, which results in side effects that can harm the metabolism and the drug material is wasted. Oppositely, after a period of time, the concentration of the drug falls below the minimum effective level, which results in the wasting of the drug without making any effect as seen in Figure 2.1.a. Also some of the drugs such as protein based drugs, and timolol, go under first-pass metabolism in the intestinal tract or liver [7]. An ideal drug delivery system possesses two elements: the ability to target and controlled release. Targeting will ensure a high efficiency of the drug and even more important it will reduce side effects. Drugs that are supposed to kill cancer cells can also kill healthy cells when delivered to them[1]. The reduction or even prevention of side effects can also be achieved by controlled release. This case is shown in Figure 2.1.b where drug level in blood is kept at the right value.

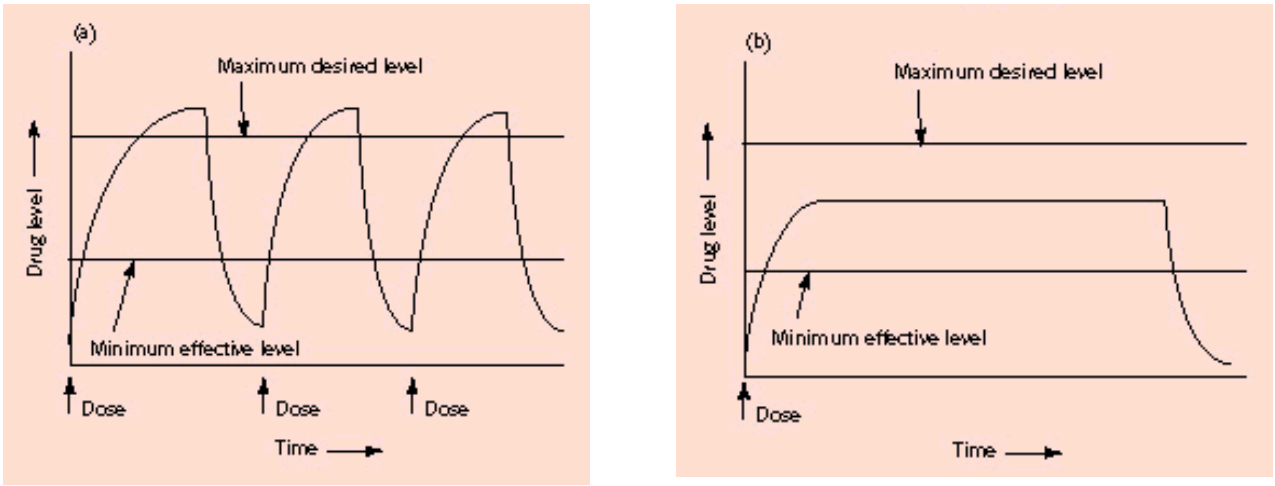

Figure 2.1 Drug level in blood for traditional (a) and controlled (b) drug delivery

[1]As one example where targeting can be important, in the UK alone there are 44,000 skin carcinoma cases per year, of which 2000 are fatal [3].

2.2. Methods of Transdermal Delivery

Human skin is virtually impermeable to molecules, exclusively to high molecular weight and non-lipophilic ones, since it basically evolved to protect the body from exterior effects. The uppermost layer, which is the *stratum corneum*, poses the greatest resistance to penetration, with its distinctive architecture and its unique nature of interstitial lipoidal environment [8].

Transdermal therapeutic systems have found wide application and gained considerable commercial success in recent years, winning the competition with other controlled drug release systems such as peroral (osmotic minipumps), parenteral (nanoparticles and nanocapsules), subcutaneous (implants), intracavitary (inrauterine inserts and various suppositoria), buccal, etc [1]. Transdermal drug delivery is a viable administration route for potent therapeutic agents which cannot withstand the hostile environment of the gastrointestinal tract and/or are subject to considerable first-pass metabolism by the liver [9]. The transdermal route can also permit the noninvasive delivery of peptide-based pharmaceuticals, if the delivery can be improved by chemical enhancers, iontophoresis, or other means [10]. The methods of transdermal delivery fall into two main categories. The first, which is the traditional delivery method, is the passive diffusion. The other methods are active in that they employ some kind of physical or chemical phenomenon in order to enhance the permeation of the drug into the body.

2.2.1. Passive Diffusion

Also referred to as transdermal permeation or simple diffusion, passive diffusion is one of the established drug delivery routes such as topical applications, ointments, and patches applied without any enhancing mechanisms. Passive diffusion offers limited possibilities, since human skin limits daily dosage delivered at around 10 mg from an acceptable sized patch [11]. Concentration gradient is the driving force for delivery in passive diffusion. Nicotine patches as an aid for smoking cessation is the most widely

known of “passive” patches. Other transdermal delivery applications in use are small lipophilic drug molecules such as clonidine, estradiol, fentanyl, nitroglycerin, scopolamine and testosterone [12].

2.2.2. Phonophoresis

Phonophoresis uses an ultrasound wave to suddenly disrupt the molecular structure of the *stratum corneum* (horny layer) of the skin and drives the drug molecules through the skin. Following disruption, *stratum corneum* restores its original configuration rapidly; however it was observed that some foreign molecules and bacteria may also penetrate along with the drug molecules. This is unacceptable. Bruising is also another common after effect which is unpleasant for the patients. These drawbacks slashed the early hopes for phonophoresis [11].

2.2.3. Electroporation

Sometimes used simultaneously with iontophoresis, electroporation is the reversible permeabilization of the cell membrane. In the case of dermal delivery, *stratum corneum* is electroporated. Cells are exposed to a very brief and high voltage which opens the cell membrane pores temporarily. Although the exact mechanism of access by electroporation remains unknown, it has been successfully applied for the transfection of DNA and macromolecules such as peptides, proteins, and other gene-based compounds [11]. Use of electroporation has been suggested for cancer chemotherapy, delivery of peptides, polysaccharides, oligonucleotides, and genes [13].

2.2.4. Iontophoresis

Iontophoresis is a noninvasive and painless means of delivering various drugs into the body [14]. Transdermal administration of drugs through the skin is assisted by electrical energy in the iontophoretic method. Iontophoresis concerns small amounts of physiologically acceptable electric current to drive charged drug molecules into the body using an electrode with the same charge of the drug, producing electrostatic repulsion. Skin is a permselective membrane with negative charge at physiological pH of 7.4 [15]. So the counterions are usually cations and electro-osmotic flow occurs

(causing a net convective flow) from anode to cathode, thus enhancing the flux of positively charged drugs. Currently the US military is trying to develop a wristwatch sized iontophoresis device that will enable monitoring of the conditions of the soldiers in the battlefield from the satellite, and deliver the required drugs and vitamins etc by a signal sent to the device [11].

In Figure 2.2.1 iontophoretic delivery system as applied to a patient is seen. In Figure 2.2.2: a) Negative electrode b) Positive electrode on top of the patch c) Positively charged drug molecules delivered to the blood circulation. A bulk fluid flow accompanies this flow, which is called electro-osmosis. In this thesis (and most of the literature), the term iontophoresis is employed so as to include the electro-osmosis phenomenon too [16].

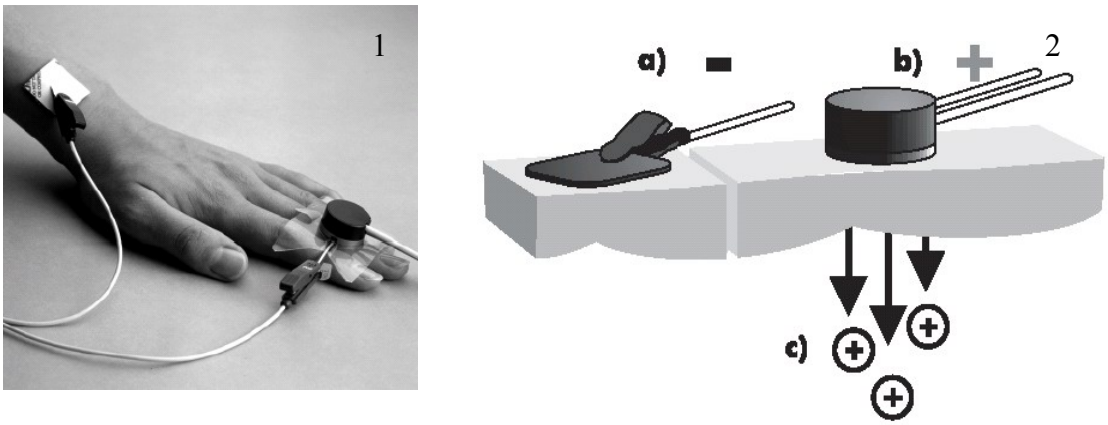

Figure 2.2 1. Iontophoretic delivery system 2. Electrode system applied to the skin surface.

The most important properties of a drug delivery patch can be listed as [16]:

1. It should be made of biocompatible material to avoid skin irritation.

2. In order to develop a patch independent of patient's race, age, or sex, the permeability of the drug through the membrane should be lower than through the skin. In this case the transdermal bioavailability of the drug becomes independent of any possible intra- and/ or inter-patient variability in skin permeability and the patch controls the drug delivery rate.

3. It should have very low electrical resistance so the overall resistance of membrane and skin during iontophoresis does not become high. A too high resistance will result in a rapid depletion of the battery. The resistance of the membranes used for

iontophoresis in our study were not high, as understood by slow depletion of the battery.

It should be noted that patch is the membrane between the skin and the drug solution here; not the drug reservoir itself. This is the same case with the SFGTA membranes of our study. The mentioned desired properties like biocompatibility, ability to control release of the drug (i.e. its permeability to the drug should be lower than that of the skin's), and low electrical resistance apply to our membrane which is not drug loaded. This is opposite of what is expected from a drug reservoir patch, which delivers the drug stored in itself. When the drug is delivered through the patch, the drug reservoir matrix or liquid solution is placed on top of the patch. In the case of delivery from the patch, the drug is loaded on the patch itself. Both cases are investigated in our study.

2.2.4.1 Previous Studies in Iontophoresis: Transdermal Patches, Ion Exchange Membranes

Controlled transdermal iontophoresis by ion-exchange fiber have been studied [7, 18]. When the membrane acts as an ion-exchange fiber, there are mobile ions like Na^+ or Cl^- introduced into the system. These mobile ions remove the charged drugs bound to the ion exchange groups of the fiber. The advantage of the ion-exchange is that it enables greater control over the delivery than systems that deliver from a drug solution with the membrane placed in between. In this study, several drugs, most of which are cations (TM is not included), have been loaded onto ion-exchange fibers and their delivery investigated. Mathematical modeling of the delivery has been performed by classical transport equations after making some sound assumptions and simplifications. Lipophilicity and hydrophilicity of the drug are other factors in drug delivery. Among the drugs studied in this study [18] tacrine and propranolol are lipophilic while nadolol is relatively hydrophilic. As a comparison, TM is a hydrophilic compound. The equilibrium distribution of the drug between the fiber and the solution phases results from both electrostatic and hydrophobic interactions. The chemical partition coefficient measures the tendency of the drug to pass to the hydrophobic fiber. As a result, it is proven that changing the (ion-exchange) fiber properties and the

external solution can control delivery. The external solution mentioned is the bathing solution for which the drug delivery is investigated. This is not the same with our system but the rule of salt concentration effect applies to our receptor solution too since the mobile ions' concentration is important there. This phenomenon of ionic strength is a parameter in the delivery of TM.

Influence of ionic strength in the adsorption and dissolution medium have also been investigated [19, 20, 21]. The membrane used was poly(acrylic acid) grafted poly(vinylidene fluoride) (PAA-PVDF). The cation exchange process of the propranolol-HCl was found to be effected by ionic strength. It was found that the low molecular weight drugs' delivery performance diminishes by increase in ionic strength; on the contrary, high MW drugs' deliveries were enhanced. Spectroscopic analysis of timolol concentration was carried out. Timolol was also investigated for comparison with propanolol-HCl.

Transdermal iontophoresis of tacrine loaded onto a commercially available ion-exchange fiber which was tested *in vivo* on human volunteers using silver/silverchloride (Ag/AgCl) electrodes [22] and the reliability of *in vitro* studies have been questioned using excised skin membranes by observing the release of levodopa and metaraminol using ion-exchange fibers [23]. Effect of pH and ion-exchange groups was found to have a great effect on the deliveries of these drugs. It was stated that studies performed using excised calf skin may not properly simulate the real *in vivo* delivery results since the epidermis layer of the excised skin is usually absent or damaged. This leaves back only the *stratum corneum*, which is stated not to govern delivery for most of the time and consequently the patch itself is controlling delivery. This can be misleading and even dangerous.

2.2.5. Selection of Electrodes

The reason for choosing Ag/AgCl electrodes is that these electrodes do not cause pH shifts as the Platinum (Pt) electrodes do [22, 7]. On the other hand, Pt electrodes can be used for changing pH when desired. Commercially available electrodes were used in our study. The phosphate buffered saline containing 6.22 g/l NaCl favours the electrode reactions in addition to making the solution isosmotic [24].

CHAPTER 3

DRUG RESERVOIR MATRIX: PREPARATION OF INSOLUBLE SILK MATRIX

3.1. Silk Fibroin

Silk is produced by arachnids (spiders) and insects as a building material for cocoons, webs etc. [25]. In Figure 3.1.a the cultivated larvae of the moth *Bombyx mori* (domestic silkworm) is in the process of producing the type of silk that is of interest to us in our research. After the cocoon is finished (Figure 3.1.b), a handful of cocoons are reeled to make the well-known silk thread as seen in Figure 3.1.c.

Figure 3.1 a) Domestic silkworm building its cocoon b) Finished cocoon c) Reeled silk

Silk has been used traditionally in the form of thread for thousands of years while there is a growing tendency to view silk as a functional material rather than a textile material in recent years [26]. Silk derived from silkworm *Bombyx mori* is a natural macromolecular protein that is made of sericin and fibroin proteins [27]. Fibroin, which is the main component of silk, is a fibrous protein that forms the thread core. The gummy amorphous protein sericin surrounds the fibroin fibers to cement them together [28]. After the sericin is removed by methods explained below, a structure consisting of fibroin remains. Repeating basic unit of Gly-Ser-Gly-Ala-Gly-Ala amino acid sequence forms fibroin structure, a high content of Gly-Ala-X repeats giving rise to the crystalline nature of silk fibers [4]. X is usually serine and it can be replaced by any other amino acid in the composition of silk fibroin (listed in Table 3.1)

[29, 30, 31], except proline [32]. The highly repetitive sections are composed of glycine, alanine and serine (approx. 85% in total) in a rough 3:2:1 ratio and the amino acid sequence is expressed roughly as Gly-Ala-Gly-Ala-Gly-Ser [33]. Freddi et al. has studied the dissolution of silk fibroin in a solvent [31]. For time zero in the dissolution, amino acid percentage given is that of native silk fibroin. A portion of the amino acid sequence of silk fibroin produced by *Bombyx mori* has been identified [30]. The crystalline region of silk fibroin is reported to compose mainly of the repetitive element Gly-Ala-Gly-Ala-Gly-Ser, and in the amorphous domain of silk fibroin is found the amino-acid sequence Thr-Gly-Ser-Ser-Gly-Phe-Gly-Pro-Tyr-Val-Ala-Asp-Gly-Gly-Tyr-Ser-Arg-Arg-Glu-Gly-Tyr-Glu-Tyr-Ala-Trp-Ser-Ser-Lys-Ser-Asp-Phe-Glu-Thr.

Table 3.1 Amino-acid content, g/ 100 g fibroin

Amino acid	Mukhamedzhanova et al.[29]	Li et al.[30]	Freddi et al.[31]
Lys	**0.51**	**0.63**	**0.33**
His	0.30	ND	0.20
Arg	1.00	0.95	0.62
Asp	2.43	2.75	1.65
Thr	1.25	1.09	0.96
Ser	**13.18**	**9.91**	**11.48**
Glu	2.09	1.30	1.37
Pro	0.53	ND	0.67
Gly	**33.34**	**35.08**	**43.68**
Ala	**26.61**	**30.75**	**29.34**
Val	2.62	4.26	2.23
Ile	0.87	1.59	0.66
Leu	0.67	1.05	0.58
Tyr	11.42	8.03	5.30
Phe	1.2	1.24	0.73
Met	NR	1.37	0.10
Cys	NR	ND	0.10

ND: Not detected NR: Not reported

Figure 3.2.a shows the polypeptide chains forming antiparallel β pleated sheets in which the chains extend parallel to the fiber axis. *Bombyx mori* silk contains at least two major fibroin proteins, light (25 kDa) and heavy (325 kDa) chains [34]; while various figures are reported for the average molecular weight like 350 kDa [5]. Actually, it was reported that upon dissolution, native fibroin which possesses light (25 kDa) and heavy (350 kDa) chains, decomposes to a mixture of polypeptides of various

sizes [28]. This is significant information considering the N *termini* of the chains play important role in intermolecular interactions. The variety of the amino acids supplies many reaction sites such as amino, carboxyl, phenol, and imidazole groups [5]. Lysine residues and N-terminal of chains are the primary source of amino groups. Free amino groups are also found on the histidine, arginine, and tryptophan amino acids [35]. These groups have significant potential for any probable interactions such as crosslinks or electrostatic interactions. It is reported that silk fibroin has many hydroxyl residues e.g., Ser 10.6 mol%, Tyr 5.0 mol%, and Thr 0.9 mol% although carboxyl and amino group content was actually low (3.9 mol%) based on the amino acid composition of silk fibroin [36].

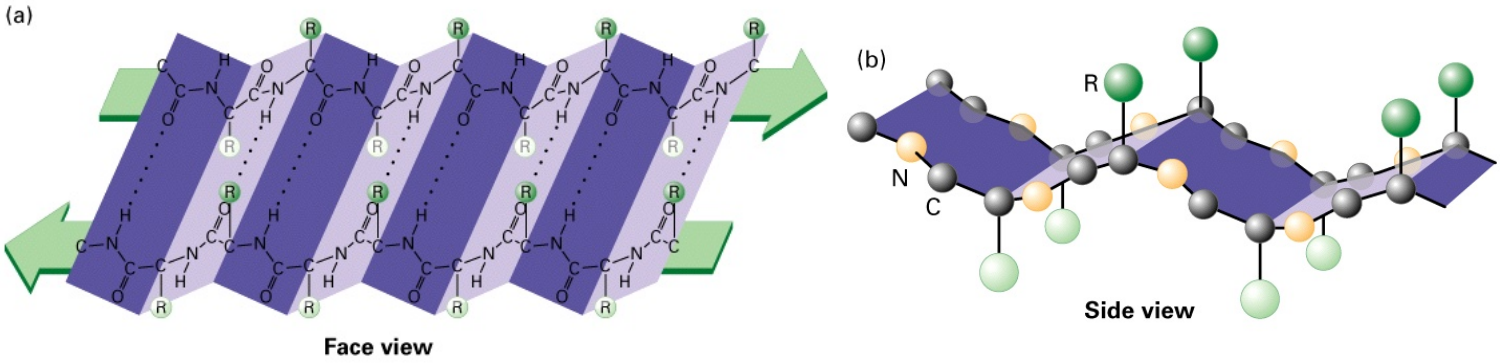

Figure 3.2 β pleated structure of silk fibroin a) Face view b) Side view

The Gly side chains extend perpendicular from one surface while its Ala or Ser side chains extend from the other surface (Figure 3.2.b). Hydrogen bonds lie within the plane of the sheet. These polypeptide chains are almost fully extended, so silk fibers are only slightly extensible, though strong. However the β sheets interact with each other only through weak Van der Walls forces [29], rendering the fibroin flexible. Along with the pleated β sheet structure, there are also amorphous regions in the fibroin in which bulky residues of Tyr, Val, Arg and Asp occur. The amorphous region enhances extensibility while diminishing elasticity [25]. The silk film cast from aqueous solution consists of two structures: the α-form (or silk fibroin I) and the β-form (or silk fibroin II) [37].

Recently, several researchers have investigated the silk fibroin (SF) as one of promising resources of biotechnology and biomedical materials due to its unique

properties including good biocompatibility, good oxygen and water vapor permeability, biodegradability, and minimal inflammatory reaction [6], microbial resistance [4], blood compatibility [26]. Some of these functionalities of fibroin were attributed to the amorphous and not the crystal region of fibroin and a fractal approach was developed to explain penetration of water vapor into regenerated silk fibroin [26]. This region is responsible for the elasticity of silk compared to fibers of similar tensile integrity, and although US Pharmacopeia lists silk as non-biodegradable since it does not "lose most of its tensile strength within 60 days", it is actually degradable over longer periods by the proteolytic degradation mechanism [34]. SF in regenerated forms has been used as surgical sutures, food additives, and cosmetics, and using of SF has been proposed for many purposes such as drug delivery (controlled release [34], a carrier of controlled release medicine [30]), soft contact lenses with high oxygen permeability, wound protection, substrate for cell culture, and enzyme immobilization [4]. Silk fibroin-based wound dressing was developed that could accelerate healing and could be peeled of without damaging newly formed skin; and it was also reported that silk fibroin membrane can be used to preferentially remove water from a mixture of water and alcohol [27]. Fibroin has also certain nutrient value to humans [5]. Uses of silk as burn wound dressings, templates for osteogenic tissue formation were listed in a study that investigated a silk-fiber matrix as a suitable material for tissue engineering anterior cruciate ligaments (for knee joints) [38]. It is an interesting point that hyaluronic acid is a major component of the synovial fluid which lubricates the knee joints. The interactions of SF and HA can draw interest from this aspect too. Silk fibroin is reported to have been blended with cellulose, PVA, polyurethane, cellulose acetate, chitosan, sodium polyglutamate, polyethyleneglycol (PEG) [39], sodium alginate, and *S*-carboxymethyl keratin [40].

Silk fibroin contains disulfide crosslinks among its heavy and light chains; however these do not normally participate in intramolecular reactions [41]. Cysteine residues of the silk fibroin may be attempted for such a modification, though there are few studies about this in literature [42].

Silk fibroin has high versatility that it can be processed into foams, films, gel, powder, fibers and meshes with good strength [5, 34]. Pulverized fibroin has also been

commercialized [43]. SF powder has been used in the production of hydroxyapatite-SF nano-composite sol for the purpose of producing artificial bone or dental roots [44].

3.2. Methods of Silk Fibroin Matrix Preparation

Silk fibroin films prepared by casting the aqueous protein solution and drying at 25 ^{o}C as seen in Figure 3.3 are soluble in water. Such films have a micro phase-separated structure consisting of crystal and amorphous regions [45]. These films should be fixed with physical or chemical crosslinking. Bifunctional agents such as glutalaldehyde are usually used for crosslinking. However, unreacted glutalaldehyde remaining in the structure is cytotoxic.

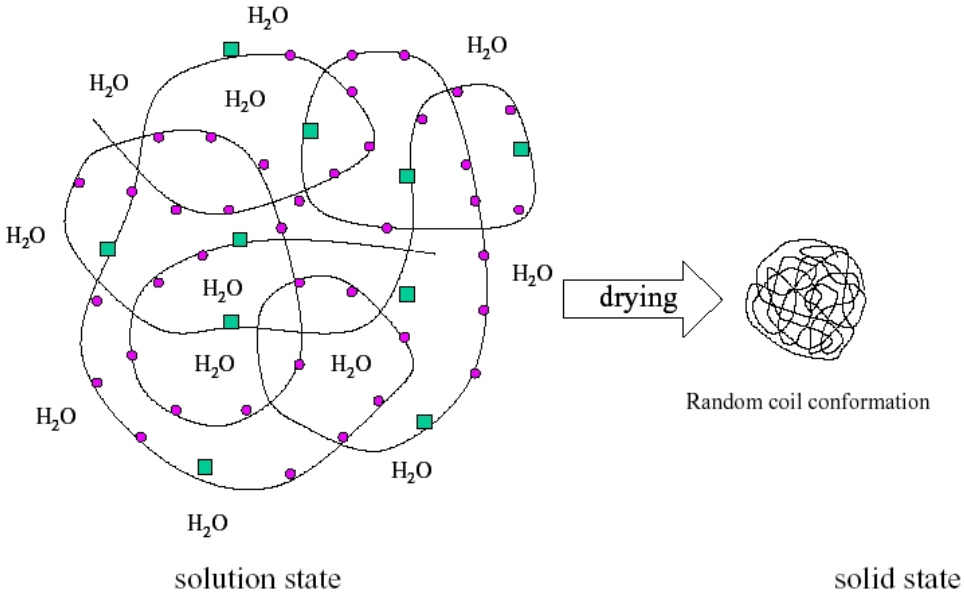

Figure 3.3 Scheme for the molecular shape of SF molecules in solution and solid state for aqueous system

Crystallization by immersing in aqueous ethanol or methanol (Figure 3.4) is another widely used method to induce structural change from random coil to β-sheet structure [46]. Degree of crystallinity increases up to 11%[2]. Methanol treatment was applied to fibroin membranes for varying intervals of 3 to 60 minutes and their oxygen permeabilities were investigated. Films were cast from 1% silk solution, dried at 25 ^{o}C and 65% relative humidity (RH), immersed in 1:1 methanol-water solution, and again

[2] It should be noted that, in literature it is also reported that β sheets are not necessarily in crystalline form [35]. That is to say, there might not be a linear quantitative relation between the crystallinity of the samples and their β sheet percentage.

conditioned at 7 days at 25 ^{o}C and 65% RH [45]. It is stated that the amorphous region of silk is responsible for oxygen permeation and duration of methanol treatment can affect this permeation behavior [47]. Zhang has used a unique and peculiar physical treatment technique to achieve anti-parallel β-sheet structure, which involves stretching, compressing and standing under high humidity [5]. The starting solution concentration is also of critical importance for the structure of the fabricated films (see Figure 3.5).

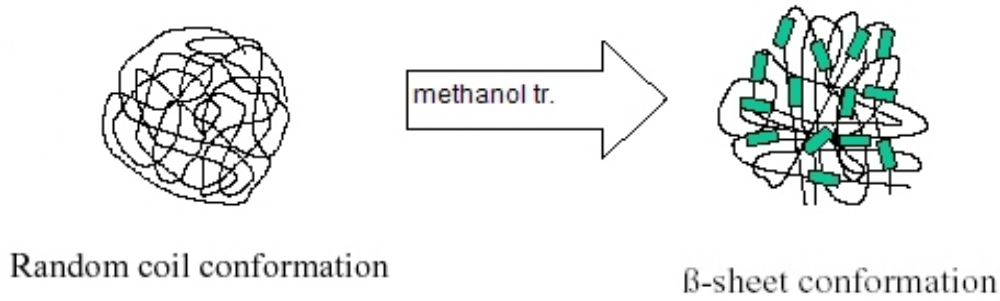

Figure 3.4 Conformation change of SF in solid state by immersion in methanol (Green boxes represent long-range ordered crystallite)

Undegraded native fibroin solution from cocoons was prepared in literature by this method: after reeling by standard methods by machine, degumming was performed in 50 times (v/w) boiling aqueous 0.05% Na_2CO_3 solution. Then the purified fibroin was dissolved in 15 times standard Ajisawa's reagent ($CaCl_2$, EtOH, water, 1:2:8 mole ratio) [28]. This is the universally accepted dissolution method which is also used in our study and elsewhere [49]. Ajisawa's and other salt solutions used to dissolve silk are referred to as chaotropic solutions (LiSCN, LiBr, NaSCN, and $CaCl_2$). The degradation of fibroin and resulting molecular weights of the protein by various treatments have been investigated, and it was found that the $CaCl_2$ treatment does not cause appreciable degradation, so it is used in this study. Removal of sericin in hot alkaline solution causes some degradation of the heavy chain of silk, so it should be performed at same time and temperature every time. This could be checked by SDS-PAGE (polyacrylamide gel electrophoresis method employing polyacrylamide gel with sodium dodecyl sulfate buffer) analysis or alternatively rheologic methods. It is also noted that the solution of intact (undegraded) fibroin has a strong tendency to gel and so it is advised that it is dialyzed just prior to use, which was experienced and practiced in our study.

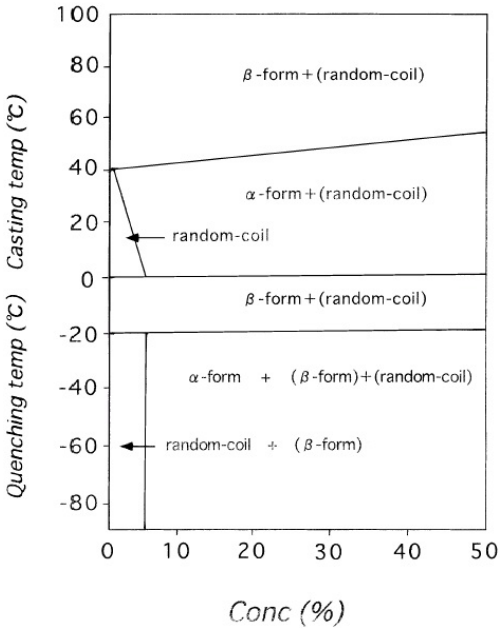

Figure 3.5 The relation between conformation, quenching or casting temperature and (starting) concentration of silk fibroin, B. mori [37]

Formic acid has also been employed as a solvent for the dissolution of silk fibroin instead of the ternary solvent of $CaCl_2$/EtOH/water [6, 35]. It has been stated in literature that dissolution of SF is desired when is used for purposes other than textile, like film, porous membrane, gel, and powder. Aqueous solution of concentrated neutral salts like calcium chloride have a tendency to become unstable and precipitation of SF is possible due to low solubility (such a phenomenon has been observed in our experiments as a small precipitate during dialysis stage). Another advantage of dissolution in formic acid is that when SF is going to be blended with other polymers, solubility of the blending agent in the concentrated salt solution is usually problematic. This is not the case with formic acid, which has been reported to be a good co-solvent for blending applications. In our case, blending of the two components SF and HA will be performed in aqueous medium employing their solutions in water. In the mentioned study, solutions of SF in formic acid and water have been studied, and also a film was also cast from the formic acid solution of SF. Although methanol treatment has been applied to the solution, it is understood that this was not applied to the cast film. Formic acid dissolution is found to create an effect similar to methanol treatment on the cast film. This effect is the conversion of the amorphous structure to a β-pleated crystalline structure, bringing insolubility in water. Structural characteristics and crystallinity have been investigated by XRD and Ft-Ir. DTA and DSC have also been

employed [6]. Solubility of the silk in water was not tested for the film, however it is discussed that in water fibroin molecules aggregate and entangle each other since SF is composed mostly of hydrophobic amino acids. On the contrary, SF in formic acid is reported to be free of aggregates and entangled structures. This is attributed to the charge repulsion effect between fibroin molecular chains since SF is positively charged in acid. In this study it is suggested that aqueous SF solution is not transparent and unstable. It is true that the solution is likely to become unstable when not handled with care; even so the aqueous SF solutions prepared by us were clear, transparent and stable at storage intervals shorter than one week.

Effect of processing temperature on the morphology of silk membranes and also methanol treatment was investigated [40]. Various processing methods used are casting followed by air-drying or freeze-drying, mechanical shearing, compression, the Langmuir-Blodgett technique, and bubble blowing. Molecular conformation of the resulting membrane can be controlled by the processing conditions such as solution concentration, solution temperature, quenching temperature, drying rate/ temperature/ and time, **the presence of an electric field**, pH, the presence of certain enzymes and the type of solvent. Increased drying temperature effect was discussed above. Effect of decreasing pH is the precipitation of the protein as β pleats. The random coils and α forms open (unfold), enabling the rebuilding of the hydrogen bonds between amino acid chains. Among these parameters, we manipulated composition and drying conditions in this study. Effect of electric field was examined by XRD at desorption (delivery) stage of the research, which caused crystallization of the membranes. Silk was taken from the gland of the silkworm in this study and also regenerated silk was used. After degumming, dissolution, and dialysis by standard methods, the membranes were cast onto Petri dishes and dried at 30 ^{o}C in air for 48 h. Subsequently, the membranes were treated with a 75 vol% aqueous methanol solution for 15 minute and dried. The resulting membranes were 15 μm thick. Films made of regenerated fibroin did not exhibit the small particles or the irregular morphology; however they exhibited grains and nanofibrils in their morphology. It is found that higher processing temperature leads the amorphous structure in the membranes to convert to β-pleated structure. This structure produces morphology with aggregated fibrils.

3.3. Previous Studies with Silk Fibroin

3.3.1. SFGTA Blends

Sufficient mechanical strength is required for most of the applications mentioned at the previous section. Nevertheless the silk fibroin is prone to get brittle in its dry state. The brittleness can be a drawback for the use of fibroin membrane as a patch in transdermal drug delivery [50]. SF was blended with other polymers in order to overcome the drawback of SF itself by improving mechanical properties [6]. For this purpose, improvements in physical properties of fibroin-based biomaterials have been sought by blending with other agents, including chitosan, sodium alginate, poly(vinyl alcohol) (PVA), and cellulose, of which PVA was found to be effective [50,4]. When blended with PVA, fibroin is said to make up a hydrogel with excellent moisture adsorbing and desorbing properties and elasticity [27]. SF/PVA blends were also used for enzyme immobilization [48]. In our study, blending the fibroin with hyaluronic acid (HA) can eliminate this disadvantage. If a cross-linking agent is used, it is in interest that this agent does not ruin the biocompatibility of the membrane. HA is similar to PVA in that both are well-known biocompatible materials which are soluble in water and have a high water retention capacity.

Porous composite membranes of regenerated silk fibroin and PVA were prepared for use as an immobilization matrix for glucose oxidase, as a glucose biosensor. Polyetyleneglycol (PEG) has been added to the casting solution to decrease mass-transfer resistance and obtain a porous structure [50]. Porous blend gels of silk fibroin-poly(vinyl alcohol) were prepared by freeze drying technique [4]. Same authors have also applied freeze drying and freeze-thaw techniques to aqueous solutions of SF to prepare porous films in a previous study. Parameters that affect the properties and structure of the film are concentration, freezing temperature, and the number of freeze-thaw cycles. The air dried gels were found to have an higher crystallinity and mechanical strength, while the freeze-dried gels have a more porous structure. As the freezing temperature was lower, the crystallinity increased. This may contribute to insolubility in water, though no mention of the solubility phenomenon is made in the study. More than 50 % PVA addition was required to improve strength. The gels are composed of wall-like material defining separated compartments.

Silk fibroin-poly(ethylene glycol) conjugate films were developed and their structure and mechanical properties were examined [51]. In order to dissolve degummed SF, a concentrated aqueous solution of LiBr (9 M) was employed in the mentioned study and then the solution was dialysed against water. PEG and SF were reacted in the aqueous solution containing 0.1 M sodium borate as modifier. After the reaction took place, the eluate of SF-PEG was collected, unreacted materials and modifier removed accordingly, and solution was brought to 1% (w/v). The membranes were cast on polyethylene films. An SF film having a β-sheet structure was prepared by immersing the film in a 50% (v/v) methanol-water mixture for 4 h at room temperature and drying the immersed SF film at ambient relative humidity at room temperature (methanol treatment). DSC tests were performed. Circular dichromism (Cd) spectra results indicate a random coil conformation with small amounts of β-sheet and helix structures for the SF film. The methanol treated SF film exhibits only an endothermic peak at DSC, while the untreated film has an exothermic peak at 228 ^{o}C attributed to the transition from random coil to β-sheet.

3.3.2. Freeze-Dried SF

In literature porous silk fibroin material has been prepared by a freeze-drying method [52**],** and its enzymatic degradation was investigated [30]. This method produces porous, spongy structures with a high surface area. SF was also blended with PVA and freeze-dried as mentioned above.

3.3.3. SF Film with Glutaraldehyde

SF membranes are usually fixed by crosslinking with glutaraldehyde (GTA). Although the exact mechanism of protein cross-linking with glutaraldehyde is not yet clearly defined, certainly the ε-amino groups of the lysine residues and the N-terminal amino groups of the proteins are involved and there is not an absolute method to determine the degree of crosslinking for GTA [53]. Lysine residues make up of 0.5-0.6% of the amino group composition of SF (Table 3.1). Seves et al. fixed silk fabric samples with a 2.5% GTA solution [43]. GTA crosslinking of dermal sheep collagen was

performed and compared with the new method of successive epoxy and carbodiimide cross-linking [54]. Enzymes are usually immobilized in protein materials such as the silk fibroin using GTA, however methanol treatment was reported to yield better results in terms of the immobilized enzyme sensitivity [48]. The reason for using GTA films for drug loaded films and membranes without drug in this study was that TM dissolves in polar solvents such as ethanol or methanol. GTA crosslinking provide our membranes sufficient mechanical strength for iontophoretic experiments. Another alternative could be using heat treatment method. This could be applied to incorporate drugs into an insoluble film structure. Heat treatment has some disadvantages. The films acquire wrinkles and even small cracks due to very rapid drying. Fabricated structure is not perfectly standardized. Same standardization problem can be observed for methanol treatment.

3.3.4. Other Studies with Silk Fibroin

Permeabilities of ions such as KCl, K_2SO_4, K_2HPO_4, $MgCl_2$, $CaCl_2$, and $MgSO_4$, across silk fibroin membrane were measured as a function of concentration of external solution in the system of silk fibroin membrane-electrolyte solution. The SF films are known to have amphoteric properties with the positive and negative charged groups they bear [55, 56]. Silk fibroin membrane was also investigated for fluoracil drug [57]. The weak acid and base groups are amino and carboxyl groups respectively. The silk fibroin membrane is reported to have an isoelectric point about pH 4.5. This dictates that our fabricated SFGTA membranes act as cation exchanger at the subject pH of 7.4. Silk fibroin has a positive charge at this pH. Transport of pharmaceuticals through the membrane was investigated in the pH range from 3.0 to 9.0. The positively charged pharmaceutical was excluded from the membrane below the isoelectric point [58].

3.4. Hyaluronic Acid

Natural polysaccharides, such as chitin, chitosan, cellulose, hyaluronic acid, have recently been re-evauluated and found to be useful resources and functional

materials. The homopolymers of were polysaccharides inadequate to meet the diverse demands for materials, so they are blended with other polymers [59]. Hyaluronic acid (HA) is a linear acidic polysaccharide consisting of alternating units of D-GlcA and D-GlcNAc: [→4)-β-D-Glc*p*A-1→3)-β-D-Glc*p*NAc-(1→]*n*, (Figure 3.6). Alternating disaccharide units of N-acetyl-d-glucosamine and d-glucuronic acid are joined by alternating β-(1–3) glucuronidic and β-(1–4) glucosaminidic bond [60]. It is a major component of the extracellular matrix of connective tissue and is found in high concentrations in umbilical cord, vitreous body of the eye, and in synovial fluid. HA is quite distinct from other glycosaminoglycans. All carry sulphate groups and their polysaccharide chains are relatively short (<100 kDa). To the contrary, it is the only non-sulfated glycosaminoglycan (GAG) in the extracellular matrix [61]. This means the primary structure of HA contains neither sulphate groups nor peptide as it is not covalently bound to proteins [62]. Although it consists of a single polysaccharide chain like other glycosaminoglycans, HA usually has a high molecular weight (10^5–10^7 g/mol) depending on the length of the chains [63].

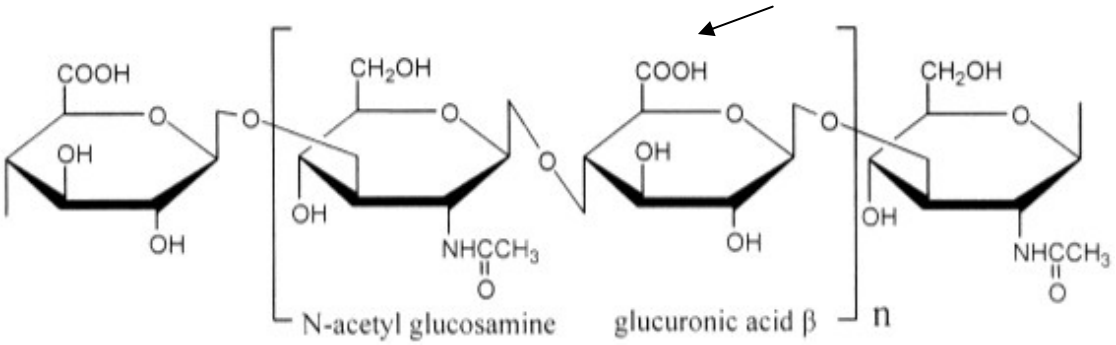

Figure 3.6 Chemical structure of hyaluronic acid [64] (arrow indicates carboxyl group)

HA possesses a high density of potential hydrogen-bonding sites, but in addition, it is a **strongly polyanionic** molecule due to Na^+ or K^+ ions complexed between polysaccharide strands. It is a weak polyacid, as only one charge can be present for each density for two residues in its repeating unit [65]. HA can adopt a number of distinct double helical conformations in a variety of packing arrangements as a function of its hydration, ionic environment and temperature [66]. A typical HA strand is shown in Figure 3.7. This strand adopts secondary structure in aqueous solution, and because of the hydrogen bonding which gives stiffness to its chain, it behaves as expanded random coil with a diameter of 500 nm. The chain becomes entangled already at low concentrations in the order of 1 g/l [67].

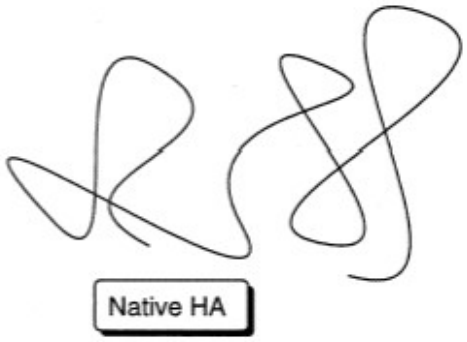

Figure 3.7 Structure of HA in its native form [70]

The attention devoted to HA in the biomaterials field has been motivated based upon its specific chemical properties. It can be functionalized with reactive groups, undergo cross-linking reactions and produce materials in the form of hydrogels [68].

Its immunoneutrality makes HA an excellent building block for biomaterials to be employed for drug delivery systems [69]. Since HA is biocompatible and biodegradable, it has been popularly used as temporal scaffolds for tissue engineering or drug delivery devices for therapeutic agents. HA was cross-linked to form a three-dimensional chain network (hydrogel) after chemically modifying HA with cross-linkable functional groups. A wide variety of polyfunctional cross-linking agents were used to form the hydrogel structure [71]. HA has been used as, a viscoelactic biomaterial for medical purposes, in cosmetics thanks to its high water retention capacity, and in drug delivery systems thanks to its biodegradability [72]. Polymer-drug conjugates for controlled release, crosslinking into hydrogels, and surface coating uses of HA was also summarized [61].

3.5. Previous Studies with Hyaluronic Acid

Prestwich et al (1998) [73] gives short but valuable insight about the drug delivery uses of HA after providing some general information about HA. The uses of HA in drug delivery started as and adjuvant for ophthalmic drug delivery and etc.

Table 3.2 Some of the related companies with HA or HA-derived products on the market [73]

Company	Product
Anika	HA-*N*-acylurea derivatives for surgical applications, treatment of osteoarthritis, bone fracture healing
Hyal Pharmaceuticals Corp.	Combining HA with existing drugs: such as diclofenac
Seikagaku Corp.	HA-enzyme conjugates
Telios Pharmaceuticals, Inc.	HA hydrogels for tissue engineering

HA is reported to have been blended with PVA for ophthalmic use, and with carboxymethylcellulose (carbodiimide crosslinked) for a bioabsorbable film for prevention of postsurgical adhesions, for wound-healing applications with collagen. It is understood that HA blends are proposed to be used for coatings in microspheres, which can be used for transcmucosal drug delivery (such as in nasal sprays). Several drug delivery uses of HA are listed in Table 3.2. HA was used as a drug reservoir as well. Lim et al [74] have prepared microspheres of HA and chitosan and evaluated the *in vitro* drug release properties and mucoadhesion of them. Bioadhesion is desired in drug administration through mucosal routes but not necessarily for dermal delivery.

HA has been also used as an attractive building block for new biocompatible and biodegradable polymers with applications in drug delivery. One study concerns the production of a crosslinked hydrogel [61]. Poly(ethylene glycol)-proiondialdehyde homobifunctional reagent is blended with HA (which is converted to its adipic dihydrazide (ADH) form). Drug loading onto this hydrogel was performed by *in-situ* polymerisation. This is achieved by dissolving the drug molecules in water or ethanol and then simply adding the casting solutions. (This method is same with the drug loading method used for the SF-GTA films in the current study.) The drug release was studied by cutting the drug-loaded hydrogel into small pieces to fit in the cuvette of the UV spectrophotometer. It was observed that the drugs were released to the PBS solution in the first ten minutes, following a first order kinetics.

The release of peptides and proteins from hydrated hyaluronic acid ester and partially esterified hyaluronic acid membranes have been investigated [75,76]. Although our research does not concern protein delivery, it is worth noting what affects the release of proteins to make comparisons. The fundamental motivation of choosing a model drug having similar properties with proteins was explained above. Since these molecules are inherently larger, they are highly dependent on porosity, cross-linking, pore size etc. This is evident by the abrupt change in release behaviour over narrow ranges of esterification. It is noted that constant or zero-order release of therapeutic agents is desirable, while for some drugs pulsatile release is desired. These studies concern the development of implantable controlled release matrices. One important criterion for these matrices is biodegradability in order to rule out the need for surgical removal.

A scaffolding material for tissue regeneration has been investigated [69]. This is a porous matrix of hyaluronic acid (HA) and collagen prepared by a freeze-drying technique. Collagen to HA ration is 8:2. HA used has molecular weight of 120-150 kDa. Experimental section of this study gives information about the preparation and characterization of an HA blend matrix.

Negatively charged HA has also been used for the coating of nanospheres for ocular drug delivery [77]. Sodium hyaluronate used had a molecular weight higher than 10^6 g/mol similar to the figure of our study. There is no cross-linking associated with coating, instead the nanospheres are coated by (1) chain entanglement of HA, (2) adsorption of HA, and (3) electrostatic interactions of HA and a cationic surfactant. Similar electrostatic interactions of the cationic and anionic substance are established in our study.

3.6. Insoluble Matrix Preparation

A probable route of interaction between HA and SF can be among the carboxyl group of the HA with the amino group of SF. This reaction can result in the formation of amide bonds. The carboxyl group can react with the amino group especially at low pH medium, where the carboxyl group is at its anion state (COO-). The stoichiometric

ratio of the amino groups and carboxyl groups were calculated. The optimum ratio of HA to SF is around 5 to 10 %. This is explained in detail in section 3.7.

3.7. Preparation of Silk Fibroin/Hyaluronic Acid Solution

In order to have an insoluble SF/HA film, it must be assured that the two molecules are incorporated effectively. The sites of modification on hyaluronic acid are the carboxyl and alcohol groups. Carboxyl groups of HA can be reduced (anions of carboxyl groups) and the amino groups of the silk fibroin can be oxidized (for example by reacting with an organic acid) (cations of amino or imino groups). This reaction scheme eliminates the need for a cross-linking agent such as glutaraldehyde.

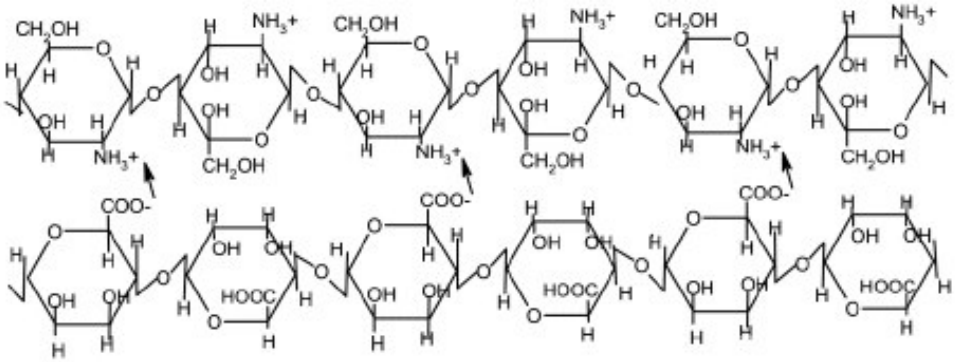

Figure 3.8 Carboxyl-amino interaction in the chitosan-alginate polyelectrolyte complex

Such an interaction is observed when amine groups of chitosan interact strongly with carboxyl groups of alginate, forming a complex (Figure 3.8). Due to the protonation amino group on chitosan and ionization of carboxylic acid group on alginate, the stability of the formed complex is influenced by environmental parameters, such as pH and ionic strength [78]. When no cross-linking agent is employed for the production of the polyion complex, this is an advantage over the blends that have been produced by making use of cross-linking agents such as formaldehyde, dimethylolurea, dimethylolethylene urea that are not biocompatible.

CHAPTER 4

LOADING AND DELIVERY OF MODEL DRUG TIMOLOL

Timolol maleate (TM) is a β-adrenergic blocking agent used in the management of hypertension and etc. It is known to undergo extensive first-pass hepatic metabolism, which makes it a potential candidate for transdermal drug delivery. The maleate salt of timolol has a formula weight of 432.5 g. The TM used in this study is in two forms: first is timolol maleate purchased from Sigma, and a 0.5% eyedrop solution of timolol. TM has an empirical formula $C_{13}H_{24}O_4N_4O_3S$. $C_4H_4O_4$. TM is widely used in iontophoretic studies [79], and it was also loaded on patches [80].

Stamatialis et al. (2002) have studied controlled transport of timolol maleate through artificial membranes under passive and iontophoretic conditions [16]. The membranes that have been investigated are commercially available membranes, which range from microporous to mesoporous. The mesoporous membranes showed no difference of transport rate with current rates. So, they are not suitable. It was understood that the molecular weight cut-off values are not a reliable way of evaluating membranes' transdermal delivery performance. The dense membranes are supposed to have a poor transport performance. However, it is of concern to investigate whether there will be any changes in structure when current is applied, or the drug molecules stuck in the film will be mobilized by swelling and the current application. The most suitable type was the microporous membrane that enabled control of TM transport by current application. This membrane has a resistance lower than skin. The type of the transport cell is not same with the diffusion cell, which was employed in our research. Adsorption to the membranes has also been investigated by dipping the membranes in a solution of TM, since adsorption can be undesirable for the purpose of use as a membrane in between. This subject was discussed in Chapter 5.

Timolol uptake and release by imprinted soft contact lenses made of N,N-diethylacrylamide and methacrylic acid (MAA) has been studied [79]. This is interesting since SF is reported to be suitable for use in soft contact lenses with high

oxygen permeability. Molecular imprinting method was employed for the production of the weakly cross-linked membrane. That is, TM was introduced into the medium while creating the membrane, in order to leave behind pores perfectly tailored for timolol. The adsorption of TM in this study gives valuable insight about the mechanism of adsorption of TM. Adsorption of TM has been fit to Langmuir isotherm. The factors affecting adsorption was investigated. These are pH, and interaction of timolol by carboxylic groups of the polymer MAA (which can be manipulated by changing composition). Timolol interaction with carboxylic groups of MAA is expected to be ionic since timolol was positively charged in the loading experiments (pK_a of protonated timolol is 9.2), and/or through hydrogen bonding with the amino, ether and hydroxyl groups of timolol structure (Figure 4.1). This information suggests that the TM may interact with carboxylic groups of the hyaluronic acid.

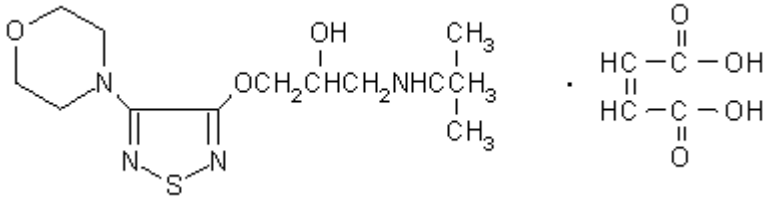

Figure 4.1 Structure of timolol maleate salt.

The imprinted gels exhibited a better performance in adsorption tests. This is related to the fact that they are weakly cross-linked compared to the unimprinted gel. It could be stated that cross-linking reduces adsorption capacity, especially when there is too much of it.

The isoelectric point of the membrane is of critical importance in the delivery of a cationic drug like TM. The isoelectric point of the SF membrane is around pH 4.0 [57]. The isoelectric point dictates that above pH 4.0, the membrane will act as a cation-exchanger and below pH 4.0 it will act as an anion-exchanger. Below the isoelectric point, cations tend to be excluded from the membrane. So, in order to control the rate of drug delivery pH can be manipulated as well as the current density. Changing the composition of the polyion complex could control the delivery behavior.

As the composition is changed, the responses of the patch to pH and current density changes could be altered.

CHAPTER 5

EXPERIMENTAL

5.1. Preparation of Silk Fibroin Solution by Ajisawa's Solution

In order to cast silk fibroin films from aqueous solutions, the preparation of the aqueous solution is handled first. Silk fibroin aqueous solution is prepared by the universally applied Ajisawa's method as mentioned in Chapter 3. This method is reported not to cause considerable degradation of the silk structure and can be used safely [28]. The aqueous solution of the silk fibroin obtained by this method is prone to get unstable (gelling) and it is preferred that it is prepared just prior to use. Preparation of silk fibroin is given in Figure 5.1.

The cocoon silk of *Bombyx mori* was obtained in reeled form from Bursa Institute for Silkworm Research. In order to assure complete removal of sericin; silk was processed three times in boiling 0.5 wt % Na_2CO_3 solution (98-100 ^oC) for 1 hour [6]. In order to avoid the water vapour bubbles to be confined in the silk structure and then burst out, large beakers (2 L) were used. The sample was rinsed with water at the end of each batch without squeezing, at the last run squeezed by hand, and dried at ventilated oven at 35 ^oC on a watch glass. The silk was now degummed (free from any sericin) and consisted of only fibroin protein.

1.5 g of the purified fibroin was dissolved in 20 times (weight/volume) ternary solvent $CaCl_2$-ethanol-water (mole ratio=1:2:8) at 78 ^oC for 2 hours with shaking in water bath. It was observed that less than 15 times solvent is insufficient to provide the physical mixing. This solution was dialyzed for 3 days at 4 ^oC in cellulose tubing with a molecular weight cut-off value of 12000 against deionized water to remove $CaCl_2$ and ions. Dialysis water was changed frequently. Fibroin molecules in aqueous solution aggregate and entangle each other by hydrophobic interactions because most of the amino acids in silk chain are hydrophobic [6], giving silk a random coil structure in water.

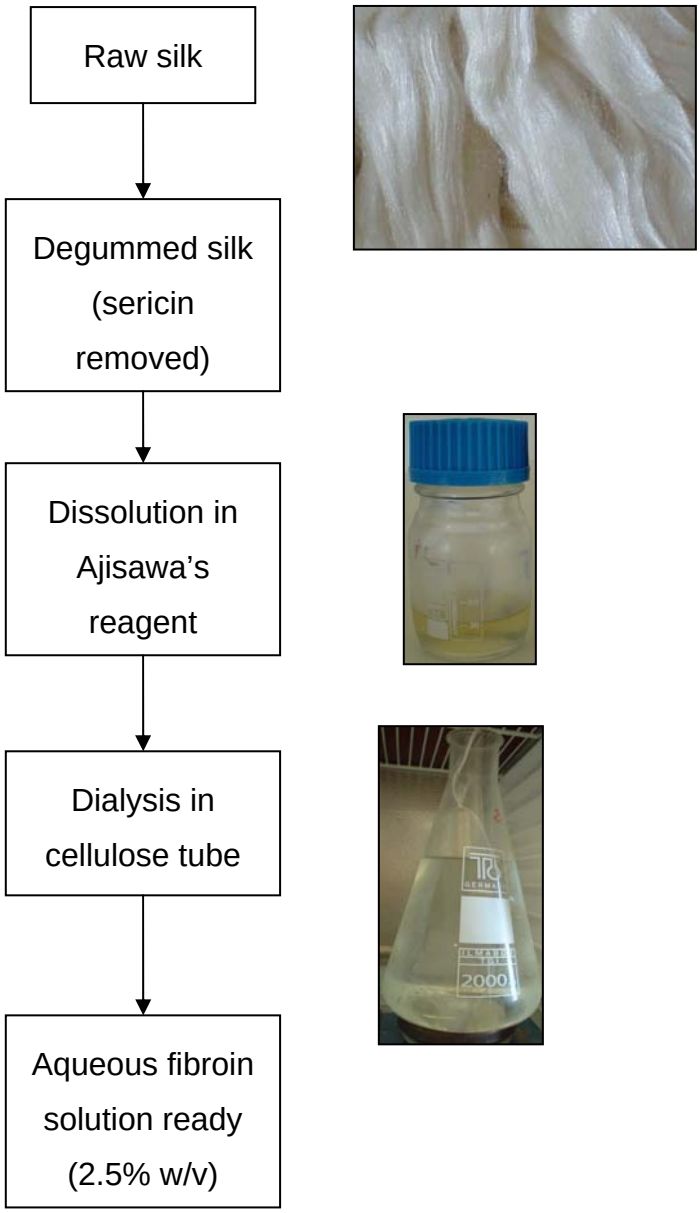

Figure 5.1 Preparation of silk fibroin solution

In order to check the removal of calcium, silver chloride precipitation test was applied to the dialysis water. After the dialysis ended, dialysis bag was taken and precipitate of silk was filtered. It was observed that the filtering of the precipitate is useful in preventing the agglomeration of fibroin molecules during the rotary evaporator step. In the presence of the precipitate, it is possible that agglomeration is enhanced by the seeding effect of the precipitate for the crystallisation of the protein molecules. The clear silk solution was concentrated to 10% (w/w) at the rotary

evaporator at 43 ^{o}C (Buchi evaporator, set T to 47-48 ^{o}C), revolutions per minute to 60 rpm. The ideal method for concentrating is slow evaporation because elevating the temperature to accelerate evaporation causes the agglomerated particles to be formed in the solution. Although it was reported that the solution can be concentrated by hanging the dialysis tube in air, in an air-ventilated room at room temperature [43], it was experienced by us that this would lead to gelling of the solution. Extended periods cause the solution become unstable and cooling can not prevent this. Actually, gelling of the solution was observed even at low temperatures like 4 ^{o}C after one month. For this reason, slow evaporation was not employed. Slow evaporation by hanging the dialysis bag at cool environment (like 10 ^{o}C) can prevent any occurrence of gelling. An alternative to eliminate the evaporation step can be to avoid the dilution of the silk in Ajisawa's solution and designing the final solution to have the desired concentration. All the same, this might cause an unstable solution.

5.2. Preparation of Drug Loading Reservoirs

The matrices to be used in delivery tests were prepared from different forms of silk fibroin and blends with hyaluronic acid and glutaraldehyde. All of these fabricated matrices are shown in Figure 5.2.

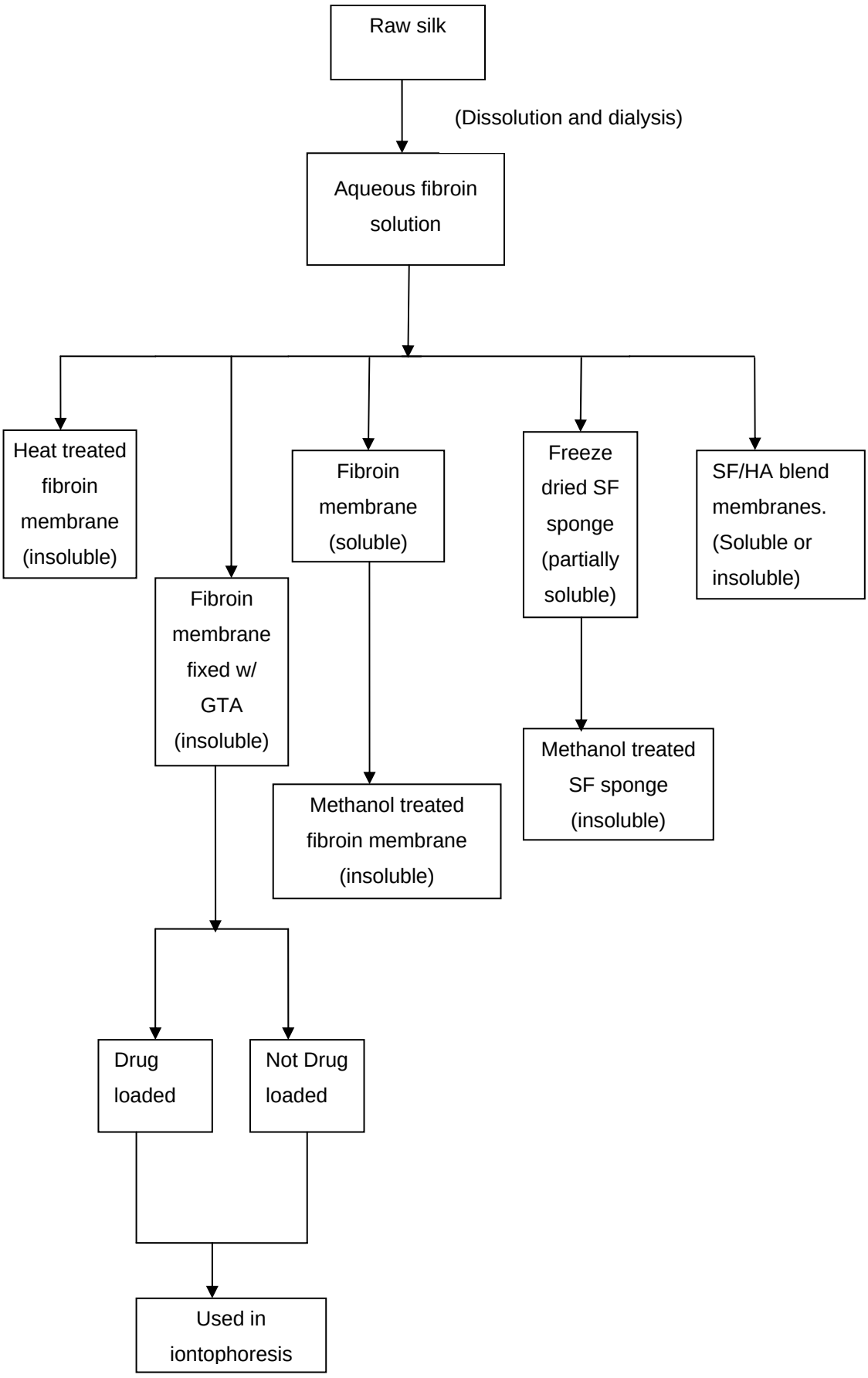

Figure 5.2 Block diagram describing various forms of SF and SF/HA blends produced in this study.

5.2.1. Preparation of Different Forms of SF

Silk fibroin films have been cast in different forms. Pure silk fibroin (SF) films, SF/hyaluronic acid blend films, and SFGTA blend films were produced. These films were dried at varying conditions. In addition, some pure SF films were subjected to post treatment in 50 % aqueous methanol. Different forms like freeze-dried fibroin have also been prepared. For the first membrane composition, which is actually pure fibroin, the 10% SF solution was cast on a glass Petri dish and dried at 30 ^{o}C in air for 48h.

Some applications of hyaluronic acid were listed in section 3.5. In order to produce a polymer matrix of silk fibroin and hyaluronic acid, the aqueous solutions of the both materials were mixed at varying proportions. The aqueous solutions were dilute, the silk solution was 10 % (w/v) while the hyaluronic acid solution was 1 %. The resulting matrices were tested for solubility in water.

5.2.1.1 Methanol Treated SF Films

After the casting of the silk fibroin membrane, it can be treated with methanol, which is known to lead to crystallinity of the structure [6]. The silk fibroin is in random coil form in aqueous medium of neutral pH. Placing the films in a 1:1 ratio aqueous methanol solution changes the conformation to an arranged state of the β sheets. An immersion time longer than 3 minutes is sufficient for the film to become insoluble in water [45]. A change to β-pleated structure enables the formation of hydrogen bonds between the adjacent fibroin chains, thus making the film insoluble in water. The films used for methanol treatment experiments were water-soluble films cast in ambient or 20 ^{o}C temperature. The solution was 50 % aqueous methanol solution. Immersion periods of 3, 6 and 10 minutes were applied. After the films were placed in small beakers, first methanol and then water was added. Films were rinsed with deionized water after treatment and left for drying at ambient temperature.

5.2.1.2 Heat Treated SF Films

For the heat-treated SF films, aqueous fibroin solution was used without concentrating. The heat treatment is known to cause the β sheet transformation to occur. The temperature of drying was 45 ^{o}C. Relative humidity was not controlled and the samples were dried at the ventilated oven for one day. The samples acquired some cracks attributed to the rapid drying. There were also ordered crinkles, which were parallel to each other. These samples were pretty brittle. Heat-treated films were insoluble in water.

5.2.2. Preparation of SF/HA Films

Our goal was to form an insoluble biocompatible matrix which has adsorption capacity for positively charged drug molecules. The agent HA is a good candidate for this purpose. 10 % SF solution was used. 1 % HA solution was prepared by slowly adding HA to deionized water while stirring vigorously. HA used in this study has a average molecular weight of 1.63 x 10^{-6} Dalton (Fluka). The compositions of the fabricated membranes and their solubility are listed in Table 6.2. The compositions of the fabricated films were designed to cover the full composition range. The pH values of the two blending agents were between 6-6.5. The mixing of two agents was achieved by using magnetic stirrer in the casting container which is the Petri dish.

5.2.3. SF Film Crosslinked with Glutaraldehyde

In order to obtain SF films with good mechanical properties to be handled in the diffusion experiments, SF films were crosslinked with glutaraldehyde (GTA). For this purpose, aqueous SF solution was used without further concentrating. Films were cast on Petri dishes of 60 mm diameter to contain a total of 0.4 g fibroin and 0.4 ml of 25% GTA solution, and dried at ambient temperature for 3 days. The thickness of the membranes was measured from SEM images. They were 90-110 μm thick.

For the preparation of drug loaded SFGTA films, same procedure was applied; with the exception that drug solution is mixed to the film during casting. The amount

of drug solution added was in the range of 40 to 150 μl. In order to prepare the membrane for diffusion experiment, a round shaped membrane with a diameter of 13 cm is cut from the mother film in the Petri dish. The mother film is soaked with 10 ml of water for 10 minutes to make it flexible and prevent cracking during membrane cutting. After the membrane is cut, it is rinsed with water and placed in the diffusion cell. Some of the loaded drug can be dissolved during this stage.

5.2.4. Freeze-Dried SF

Freeze-dried films were prepared in order to obtain high surface area and insolubility. Aqueous fibroin solution was directly used without concentrating. The freeze drier was operated between -45 and -50 ^{o}C. The pressure was not controlled and randomly assigned by the device itself, changing around minus 250-300 mm Hg. This form is denoted SFFD. The product of the freeze drying was usually slightly soluble in water. The freeze-dried sponge of fibroin was subjected to methanol treatment prior to adsorption experiments to ensure complete insolubility. This is denoted SFFD-MT. The SEM images of samples were taken. These were compared with the literature images [30]. The sponge samples for SEM were prepared with care since the sponge is very susceptible to the touch and can easily deform.

There was another sponge produced in this way: first the SF solution was poured in a Petri dish of 60 mm diameter and then placed in the cryostat for freezing. Temperature reached steady-state at -35 ^{o}C and samples were frozen at this temperature for one hour. Samples were stored at -18 ^{o}C in deep-freeze until they were freeze-dried at the same conditions listed above.

5.3. Characterization of the Membranes

The microstructures of the membranes were examined by SEM. Results were extracted about the porosity, homogeneity, and surface morphology from images. For crystallinity of the membrane, X-ray diffractometer (XRD) was used. Fourier transform infrared spectroscopy (Ft-Ir) was used to understand the chemical interaction

among SF and the blending agent HA [82]. Ft-Ir absorption bands for specific groups in the structure were analysed.

5.3.1. Solubility Tests

The solubility tests were performed by dipping the samples in deionized water and observing the state of the films visually for three days. Some of the samples were directly subjected to the adsorption tests which counted as a solubility test, and the samples which were dissolved were quickly noted and eliminated from the adsorption tests.

5.3.2. Analysis Methods

The scanning electron microscope (SEM) images were taken from the surface and cross-section of the samples by Philips XL 30S FEG. The images were used for assessment of porosity, homogeneity of blending agents (existence of separate phases), and configuration of the protein structure. Measurement of thickness and pore size were made. The X-ray diffraction (XRD) analysis gives us insight about the crystallinity of the samples. XRD analysis was carried out by Philips X'Pert Pro. This information can be interpreted by comparing the amorphous or crystalline samples, as well as any increase in crystallinity deserves attention. It should be noted that the 3 minute and 6 minute methanol treated films were ground to powder form for XRD analysis while 10 minute treated film was analysed directly. In order to confirm the crystallization of fibroin in methanol, X-ray diffractograms of methanol treated films kept in aqueous methanol for increasing intervals of time were compared. The Fourier transform infrared (Ft-Ir) spectroscopy is a powerful method to investigate the chemical bonds and interactions within a sample. Samples in membrane form were subject to Ft-Ir analysis by Shimadzu FTIR-8601.

5.4. Adsorption Experiments

Different samples prepared by different methods were tested for capability of adsorbing the model drug timolol maleate (TM). Samples were placed in dilute

solutions of TM changing between 2.5 and 5 mM. The samples were cut from the films, freeze-dried sponges, raw silk and degummed silk. The ultraviolet (UV) absorbance value is directly related to concentration of the adsorbed or released drug. The calibration curve for TM absorbance is given in Figure.A1 in Appendix A. In this study absorbance value is used for the measurement of concentration. It was required that the samples were insoluble in water since in case of presence of dissolved particles, the reliability of UV spectroscopy analysis would be reduced. The samples were kept in the adsorption medium of timolol maleate solution for 3 days at the shaker-incubator at 35 ^{o}C and 100 rpm. pH of solution was kept constant at 6.5 by phosphate buffer. Just prior to dipping in the timolol maleate solution, samples were soaked for a short time in buffer solution in order to let them absorb water. This method makes it possible to exclude the sorption and consider only adsorption. The samples taken from the adsorption medium were diluted by deionized water or buffer solution to reduce the concentration to the range of analysis by UV. Then the absorption at this concentration was corrected to actual value by multiplying with the dilution factor, subtracted from the original concentration of the stock solution. Difference gave the amount adsorbed. Results were normalized to per gram basis to make a comparison between different samples and the literature results. "Per gram" basis is more convenient than other options like "per unit area" basis since a comparable measurement of areas is not possible.

5.5. Iontophoretic Experiments

In order to test the performance of drug delivery from and through the membranes fabricated, the iontophoretic setup has been established. The main parts of this setup is the diffusion cell, the Iomed iontophoretic drug delivery device as the power supply, the UV visible spectrophotometer with the flow cell installed, peristaltic pump, and the tubings, connections etc. The schematic of the custom-made diffusion cell employed is given in Figure 5.3. The design of the cell owes inspiration to Franz diffusion cells [83]. This cell consists of two polytetrafluoroethylene (PTFE) parts joined end to end and an o-ring in between, with the membrane fixed in the middle and sealed with two gaskets. Silver/silverchloride electrodes were placed in the upper and lower compartments respectively. The cathode (Ag) is on the upper side and anode

(AgCl) on the lower side. The design of the system enables *in-situ* analysis of the amount of drug delivered to the receptor solution. This was achieved by employing a receptor solution chamber which is not very large. Diameter is 13 mm which gives an active membrane area of 1.327 cm^2. The total volume of the receptor chamber has a volume of 4.2 ml. This design ensures an undisturbed laminar flow in the receiver side. Vigorous mixing was not desirable since this would cripple the *in-situ* analysis of the drug delivery.

The drug solution used in the experiments was the eye drop of timolol (Timosol by Bilim İlaç), which is a 0.5% aqueous solution, equivalent to 0.68 mg TM per mL of drug, or the stock solution of TM (Sigma) prepared again at 0.5%. The volume of the injected drug solution was in the range of 40 μl to 1 ml.

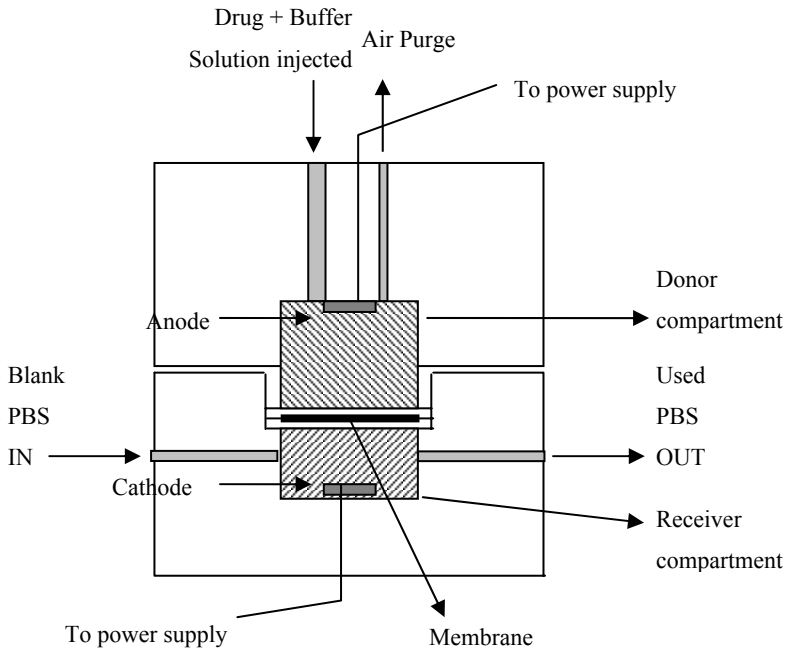

Figure 5.3 Custom-made diffusion cell used for drug delivery experiments

The diffusion cell is the heart of the experimental set-up shown in Figure 5.4. Both the inlet and outlet tubings of the iontophoretic cell were connected to the peristaltic pump. The drug solution was injected to the donor compartment and balance amount of phosphate buffered saline (PBS) solution, which contains 6.22 g/l NaCl to make it isosmotic, was added to fill the whole compartment. The fresh buffer solution

is sucked in from the PBS container. The sample then flows through the receptor cell below the membrane and is sent to the flow-cell installed in the ultraviolet-visible spectrophotometer for analysis of TM concentration. Measured concentration data were recorded continuously at the computer. The sample was collected at the effluent container after leaving the flow-cell.

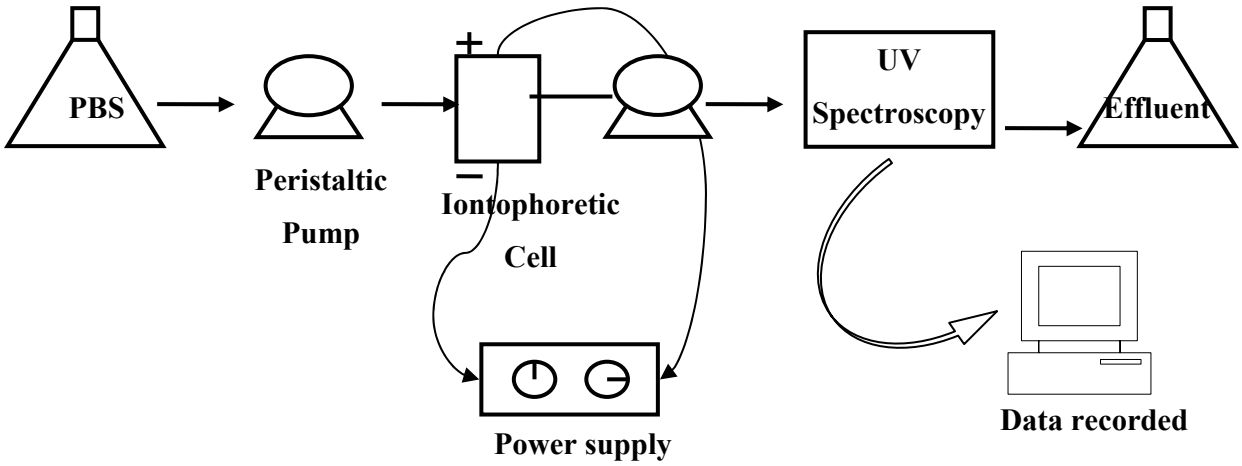

Figure 5.4 Iontophoresis experiment set-up

CHAPTER 6

RESULTS

6.1. Characterization of the Membranes

6.1.1. Effect of Post Treatment on the Structure of Silk Fibroin

The silk fibroin films cast from the aqueous solution were dried at varying conditions. The films cast at 20 ^{o}C and 45 percent relative humidity (RH) were soluble. Post-treatment with methanol was used to some of these membranes. Heat treated films were prepared by casting and drying at 45 ^{o}C. It is understood that unless an attempt was made to induce porosity in the structure, all fabricated SF films have dense structure.

Insolubilization is required for loading drug on membranes and the delivery experiments in aqueous media. Methanol treatment and heat treatment were used for this purpose on silk membranes. All of the obtained insoluble matrices are listed in Table 6.1. It was observed 3 minutes was long enough to make the films insoluble. Though both of the methanol (SFMT) and heat treated (SFHT) films possess crystalline structure, in literature grainy structure of SF films dried at high temperature is also mentioned [40]. This was also observed in this study. Methanol and heat treated films were similar in physical appearance and their outcomes in analyses. Some of heat treated films acquired cracks and wrinkles due to rapid drying. Figure 6.1 compares the morphology of methanol treatment and heat treatment on SF. The heat treated membranes also have a cross-section with varying porosity, which is attributed to the quick evaporation of the water content. The methanol treated film was dense.

It was observed that if the films were insoluble in water then they would not interact with water no matter how long they were exposed to water. In case of soluble films, it was observed that the samples were dissolved at the very first minutes of exposure. Some of the samples were dissolved partially. XRD analysis is useful in explaining if the insolubility of any subject membrane was brought about by actually

electrostatic interactions formed between or within the blended agents, or by configuration change which is dependent on drying conditions and factors like pH and ionic strength.

Table 6.1 Insoluble Samples

Sample	**Insolubilization achieved by**
Blend membrane w/ comp. 10% HA 90% SF	Interaction justified by OH stretching
Blend membrane w/ comp. 15% HA 85% SF	Interaction justified by OH stretching
Methanol treated SF film	Configuration change to β pleated structure
Heat treated SF film	Configuration change to β pleated structure
SF film cross-linked w/ glutaraldehyde	Crosslinking
Methanol treated SF freeze-dried sponge	Configuration change to β pleated structure

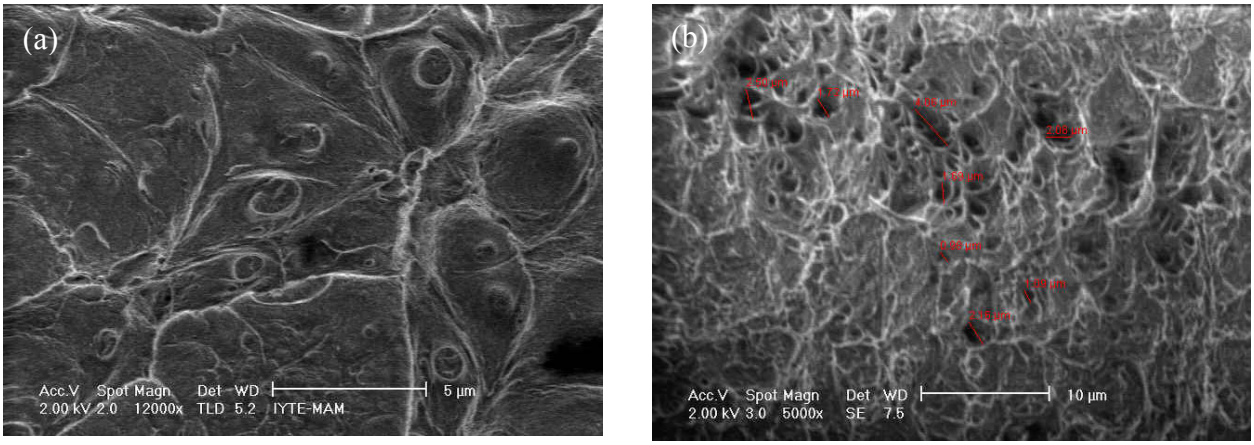

Figure 6.1 SEM image of cross-section of a) Methanol treated SF (SFMT) membrane. Magnification: 12000x. b) Heat treated SF (SFHT) membrane. Magnification: 5000x.

Methanol treated SF membrane is dense with small pits on the cross-section as depicted in Figure 6.1.a. The heat treated membrane shown in Figure 6.1.b was not as dense as other SF membranes. The reason of this could be explained by β-pleat

formation and vaporization taking place simultaneously. The membranes acquired macropores of 1 to 4 μm.

A high surface area is required to have a high drug adsorption capacity. In order to increase surface area, freeze drying of the aqueous solution of fibroin was performed. A spongy structure was obtained. Freeze-dried samples consist of a mixture random coil and β-pleated structure. This was understood by partial solubility of the freeze-dried sponge. Methanol treatment for 10 minutes in 50 % aqueous solution was applied in order to achieve insolubility. Adsorption tests yielded comparable results with literature in terms of adsorbed drug per gram of material. The freeze-dried sponge can be placed in between two layers of other membrane and used as a drug reservoir in iontophoresis. As seen in Figure 6.2.a and Figure 6.2.b, the structure was porous with a high surface area. Methanol treatment has turned the structure to a more porous form.

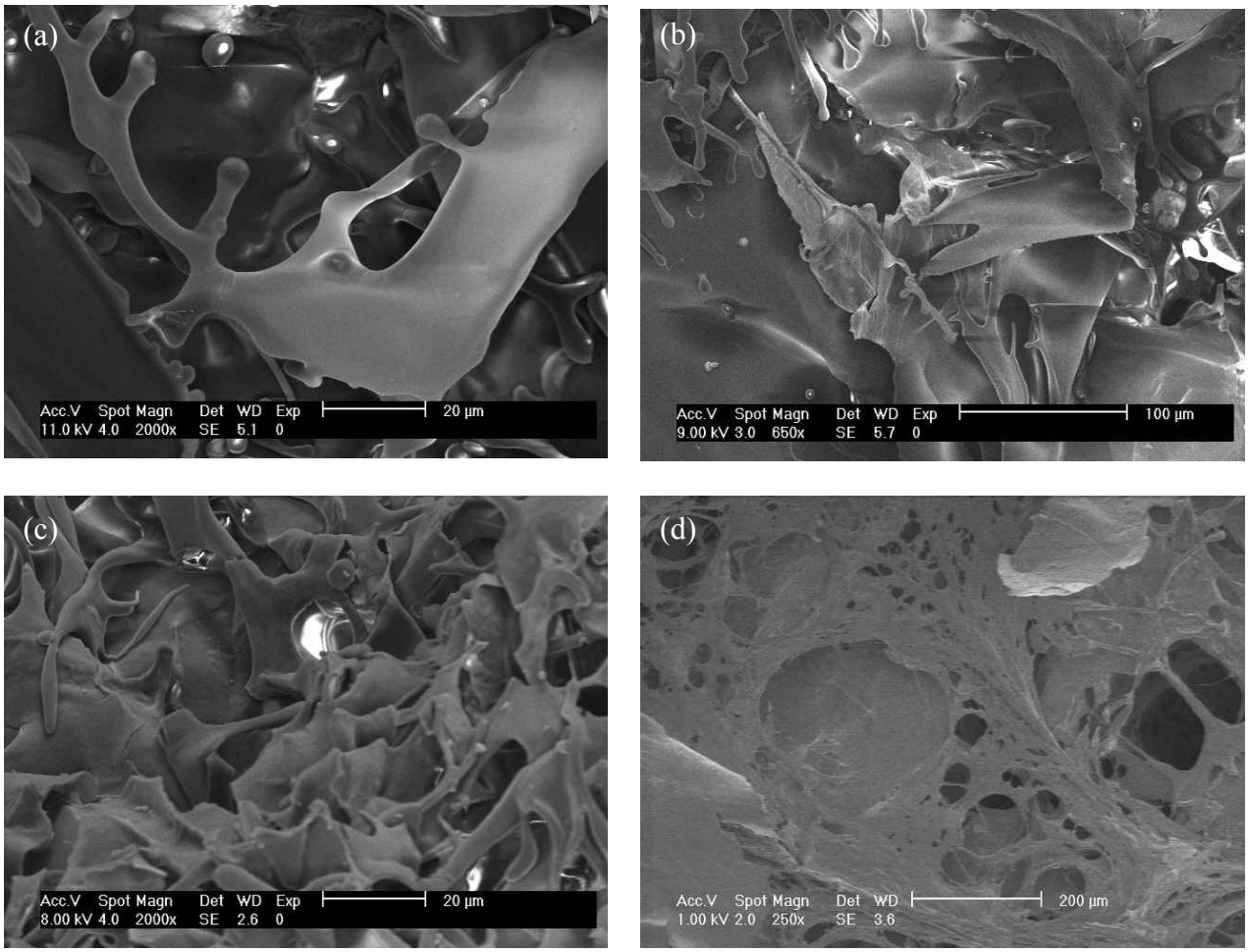

Figure 6.2 a) SEM image of freeze-dried SF sponge. Magnification: 2000x. b) Magnification: 650x. c) After methanol treatment. Magnification: 2000x. d) First frozen then freeze-dried SF. Magnification: 250x.

The freeze dried SF sponge seen in Figure 6.2.c consists of regions with low and high porosity. The samples have the well defined wall like structures and separate compartments. The samples could be compared with the literature samples of freeze dried SF by Li et al.[30], and the sheet-like structure was similar with the freeze-dried SF by Tsukada et al. [52]. Sample seen in Figure 6.2.d were first frozen and then freeze-dried. Hence it had very low density and it was weak.

To observe the effect of duration of methanol treatment, three identically formed films were treated in methanol and for 3, 6, and 10 minutes. The X-ray diffraction results are given in Figure 6.3. In Figure 6.3.a, crystallization has started, however it was not complete. This film was also insoluble though not perfectly crystalline. Its order structure makes it insoluble. This is in agreement with the literature where 3 minutes is reported to be sufficient to make films insoluble in water [45]. It is known that insolubilization can be achieved by increase in crystallinity.

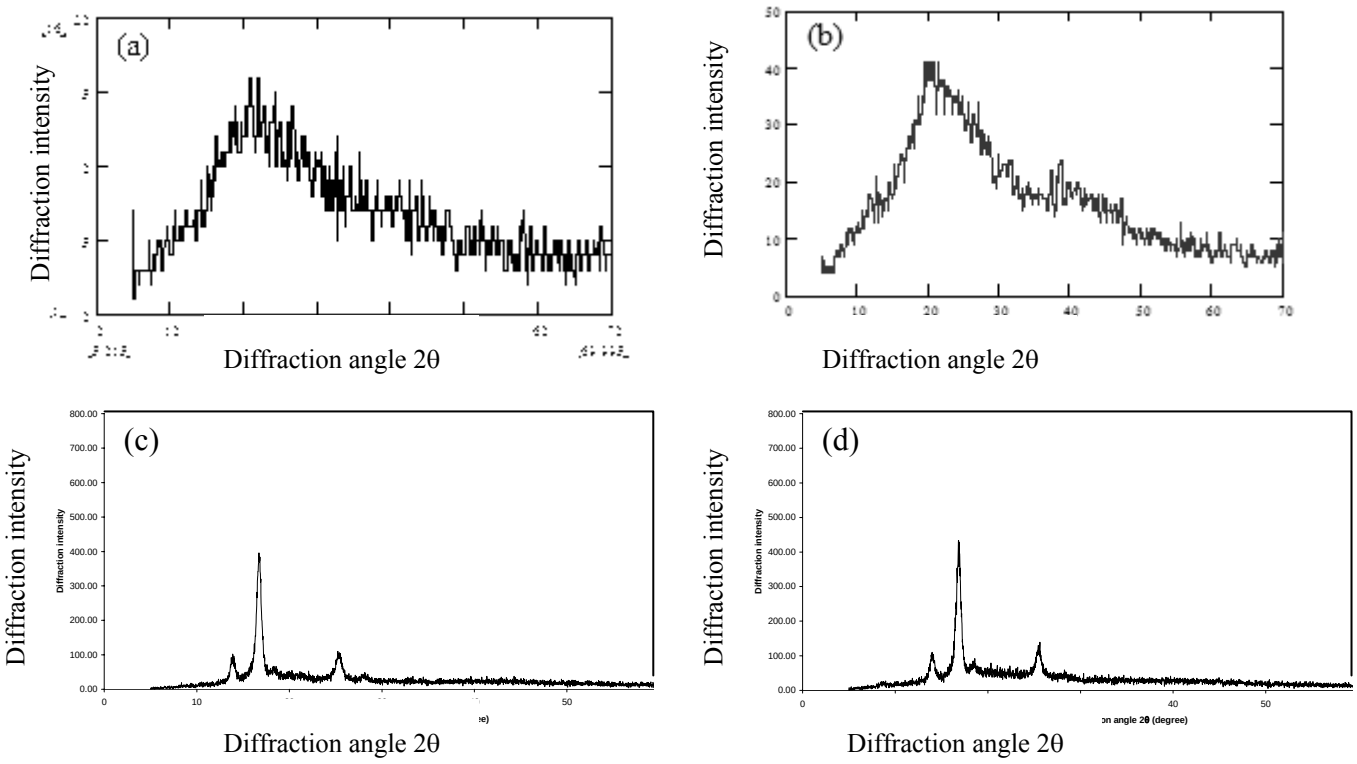

Figure 6.3 X-Ray diffractograms of SF films treated in methanol a) for 3 minutes (SF-MT 3 min) b) for 6 minutes (SF-MT 6 min) c) for 10 minutes (SF-MT 10 min) d) Heat treated SF film dried at 45 ^{o}C.

The XRD of SF-MT 3 minute depicted in Figure 6.3.a is highly irregular and noisy. In comparison, the SF-MT 6 minute (Figure 6.3.b) is more ordered and yields twice higher intensities.

The crystalline peaks and increase in intensities are visible in at XRD result of SF-MT 10 minute Figure 6.3.c. An interval of 10 minutes converts the structure to crystalline. The sample was perfectly crystalline, yielding a peak at 16.85 2θ degree with an intensity of 471. When X-ray results of SFMT 10 minute (Figure 6.3.c) and heat treated SF film dried at 45 ^{o}C (Figure 6.3.d) were compared, similar effects on the crystal structure of the films were observed. The heat treated SF film yields an XRD pattern similar to the other crystalline structures. The insolubility property and the crystal structure finding are consistent with the literature (47, 37, 40).

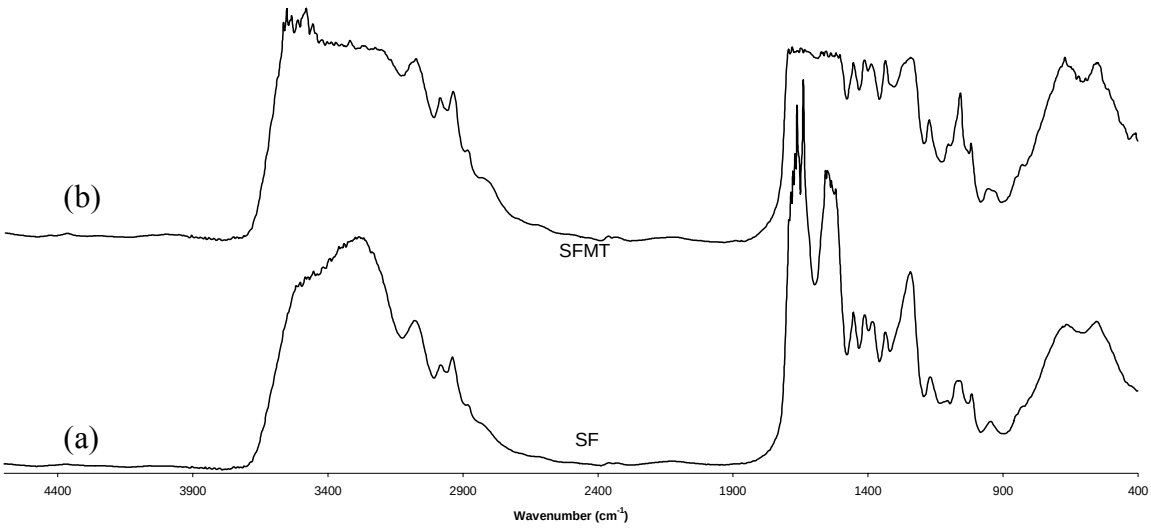

Figure 6.4 Ft-Ir spectra of a) silk film and b) methanol treated silk film.

It has been mentioned that the films cast from the aqueous solution are soluble and consist of random coil and α structures. In Chapter 3 it was stated that starting concentration and casting temperature is important for the structure of the fabricated films. When casting temperature is below 40 ^{o}C, an aqueous solution yields an SF film with α-form and random coil, which is obviously soluble. Treating in 50% aqueous methanol for several minutes convert the silk fibroin to β pleated structure. The configuration change by methanol treatment can be detected by Ft-Ir spectra results of

SF and SFMT films as given in Figure 6.4. The characteristic peak of amide I and amide II bands are between 1620-1660 cm^{-1} and 1530-1540 cm^{-1} respectively [83, 82, 85]. When SF and SFMT were compared, it was observed that the peaks attributed to both amide bonds were trimmed. That is to say, the absorbance peaks at the two amide bonds were lowered to the same intensity and became one broad peak.

6.2. Formation of SF Film

6.2.1. SF/HA Films

The weight ratios of SF and HA and solubilities of films formed are given in Table 6.2.

Table 6.2 Weight ratios of the two components in the polymer matrices.

Hyaluronic acid	Silk fibroin	Solubility
0	100	Soluble
10	90	Insoluble
15	85	Insoluble
25	75	Soluble
30	70	Soluble
50	50	Soluble
70	30	Soluble
75	25	Soluble
100	0	Soluble

These films fall into two main categories: soluble and insoluble. The solubility case might not necessarily mean that there was no interaction in the structure. The stoichiometric balance amount of HA can cross-link with SF and excess HA would be free and dissolve in water. However, there were no distinctive morphological differences between the soluble and insoluble films. All were dense and for the most part non-porous. All of the films below were around 10 μm thick. When the two solutions were mixed, their mixture became white although both of the blending solutions were transparent. Turbidity is a consequence of intense light scattering with colloidal dispersion [6]. Then our protein polysaccharide mixture of SF and HA was not perfectly homogeneous [86].

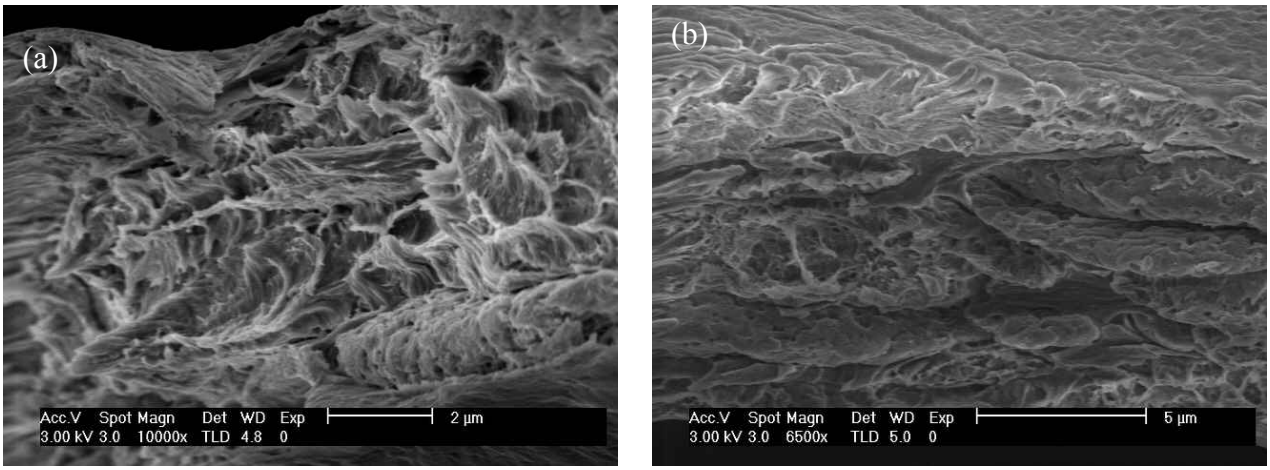

Figure 6.5 SEM image of cross-section of soluble membranes. Composition: 50% HA, 50% SF. Magnification: 10000x. b) Composition: 70% HA, 30% SF. Magnification: 6500x.

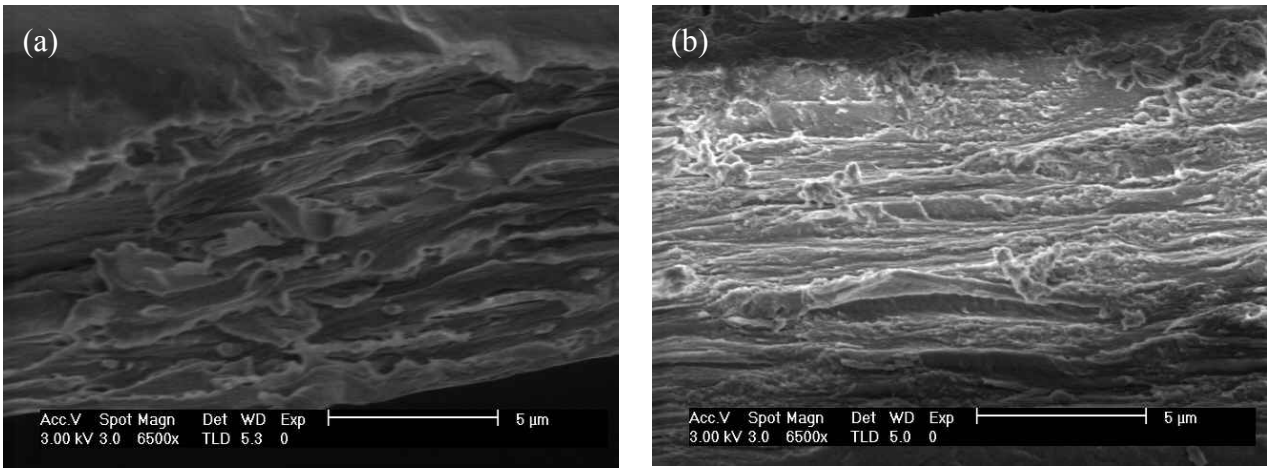

Figure 6.6 SEM image of cross-section of insoluble membranes. a) Composition: 15% HA, 85% SF. Magnification: 6500x. b) Composition: 10% HA, 90% SF. Magnification: 6500x.

The above SEM images of soluble SF/HA Figure 6.5 and insoluble SF/HA Figure 6.6 indicate that there is a tendency in the insoluble films to form sheet-like structures. This is also due to the high SF content of these films.

The X-ray diffractograms of the soluble and insoluble HA films exhibit differences in degree of crystallinity and diffraction intensity. When X-Ray diffractograms given in Figure 6.7 are examined, it could be seen both of the two

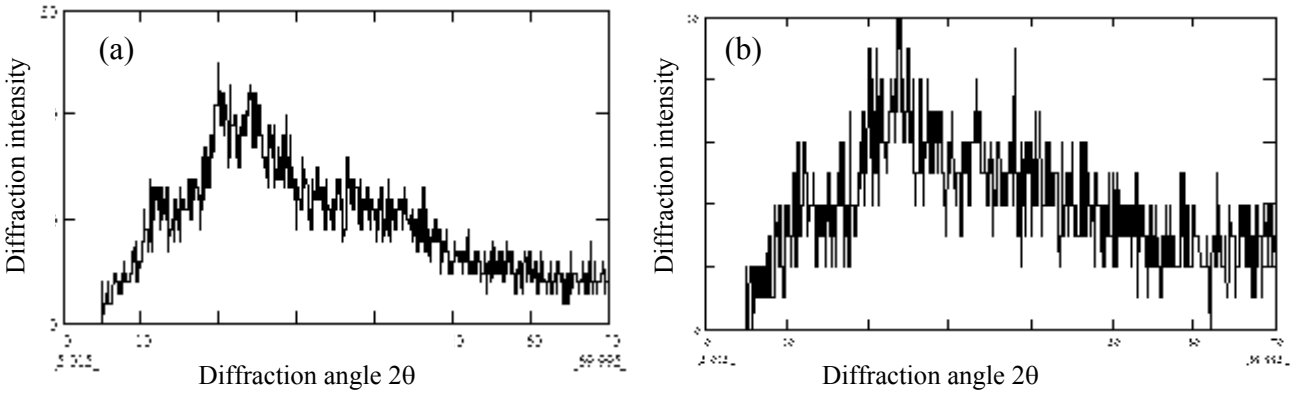

Figure 6.7 X-Ray diffractograms of a) 10% HA insoluble film (smoothed). b) 15% HA insoluble film (smoothed).

insoluble samples with 10 and 15% HA generated low diffraction intensities and irregular patterns which is a sign of amorphous structure. The XRD results of insoluble films of 50 and 70% HA also yielded amorph structure. There are differences in that the insoluble films yielded highly amorphous diffractograms while the insoluble films, whose diffractograms are given in Figure 6.7.a and Figure 6.7.b were more regular in comparison. It was mentioned that insolubilization can be established by a small increase in crystallinity. The Ft-Ir analysis below should be more useful in distinguishing whether the insolubilization was brought about by configuration change or intermolecular interaction.

Among the films produced at various blending ratios as listed in Table 6.2, films with 10 and 15 percent hyaluronic acid proved to be insoluble. The spectrum of the insoluble 10% HA film was compared with pure HA in Figure 6.8.a, pure SF (Figure 6.8.d) and the soluble 10% HA film in Figure 6.8.b. When Figure 6.4 and Figure 6.8.c are examined, it could be seen that the insoluble 10% HA film yields an Ft-Ir spectrum closer to the SF film of Figure 6.8.d, and not the SFMT film. This result indicates that the insolubilization was not related to configuration change to a β-pleated structure. This is also evident by the amorphous structure findings of XRD in Figure 6.7.a and Figure 6.7.b. The solubilization was provided by chemical interaction of HA and SF which is evident by the narrowing of the broad peak attributed to O-H stretching. Indicators of new bond formation are: i) new peak appearance, ii) shift or disappearance of existing peaks or iii) intensity increase of a band. A narrowed O-H stretching peak was observed in Figure 6.8.c. indicating an increased intermolecular interaction.

Similar results are reported in literature. Kim et al. [86] have produced polyion complex composite membranes consisting of sodium alginate/chitosan. The complexation occurs between the amino and carboxyl groups of the ionic polymers involved in this study. It is stated that as the polyion complex formation proceeded, the O-H stretching peak at 3380 cm^{-1} became narrower, which is attributed to an increase in intermolecular interaction such as hydrogen bonding between sodium alginate and chitosan. Coating achieved by electrostatic interactions between a cationic substance and HA was also mentioned earlier (Section 3.5) [77]. It is known that the presence of COOH groups in HA promote the formation of hydrogen bonds with components of the biological substrate in the body (mucoadhesiveness) [74].

It is also known that blending with other polymers like sodium alginate and chitosan can change conformation of silk [33]. The results for insoluble films could also be questioned in this aspect.

6.3. Glutaraldehyde Cross-Linked SF Film

The SFGTA film has very dense, non-porous and transparent structure. The film looks virtually impenetrable in the SEM images. SFGTA films have crystalline structure.

6.4. Adsorption Experiments

One aim of this study is to investigate the potential of SF drug reservoirs to be employed in iontophoretic delivery. The second stage of this effort is to adsorb the drug molecules onto the films. In order to investigate the TM adsorption capacity, membranes were placed in 10 ml aqueous solutions of timolol of various concentrations [79]. The pH of the solution was adjusted to 6.5-7. Samples were equilibrated for 3 days and after that, amount adsorbed was found from the difference in concentration of timolol in the initial and final solutions. UV spectrophotometer was used to measure the TM concentration in the final solution. The composition of the membrane that gives the maximum adsorption of timolol maleate was determined.

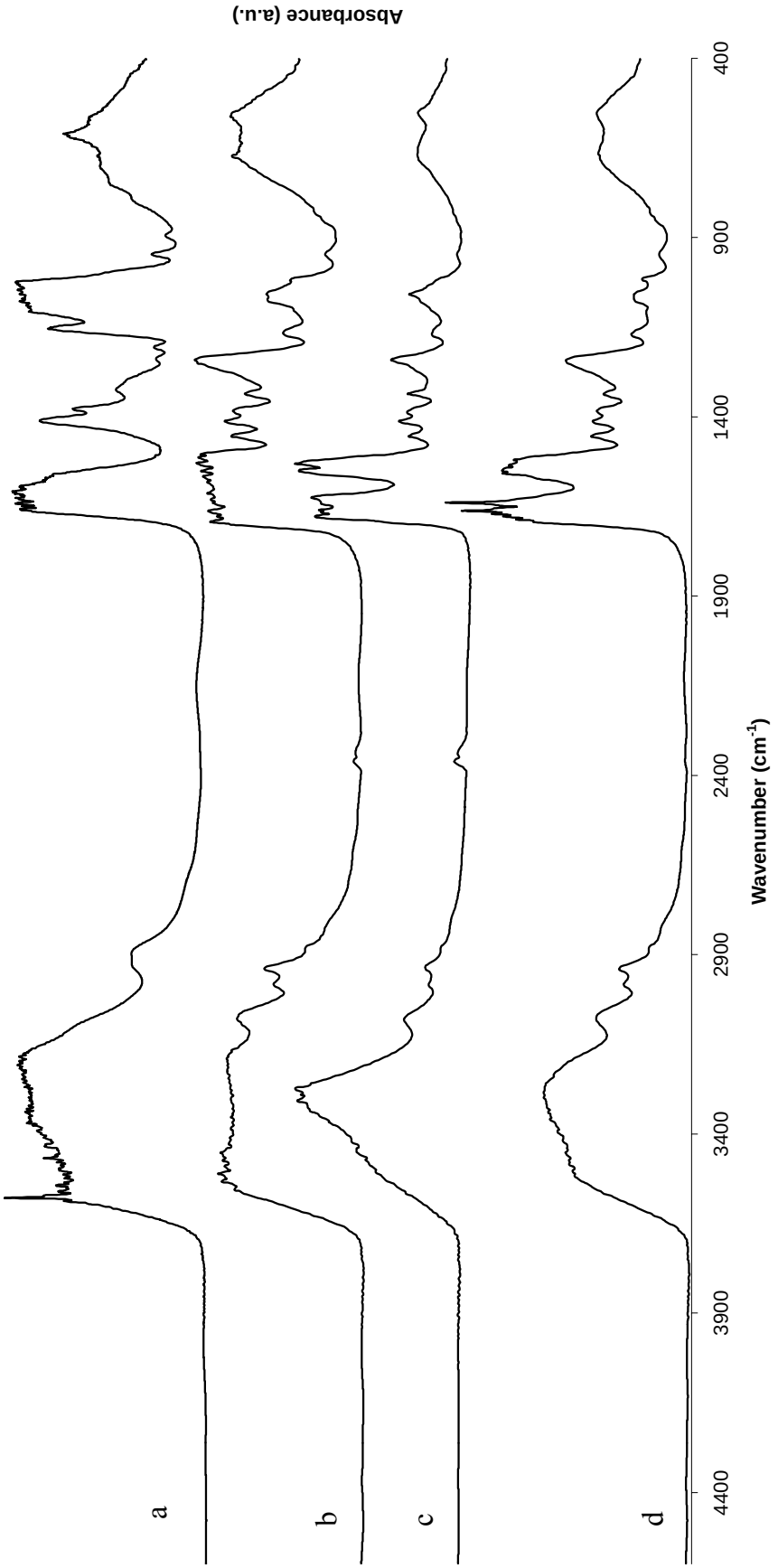

Figure 6.8 Ft-Ir spectra of a) HA film b) 10% HA, 90% SF soluble film c) 10% HA, 90% SF insoluble film d) SF film

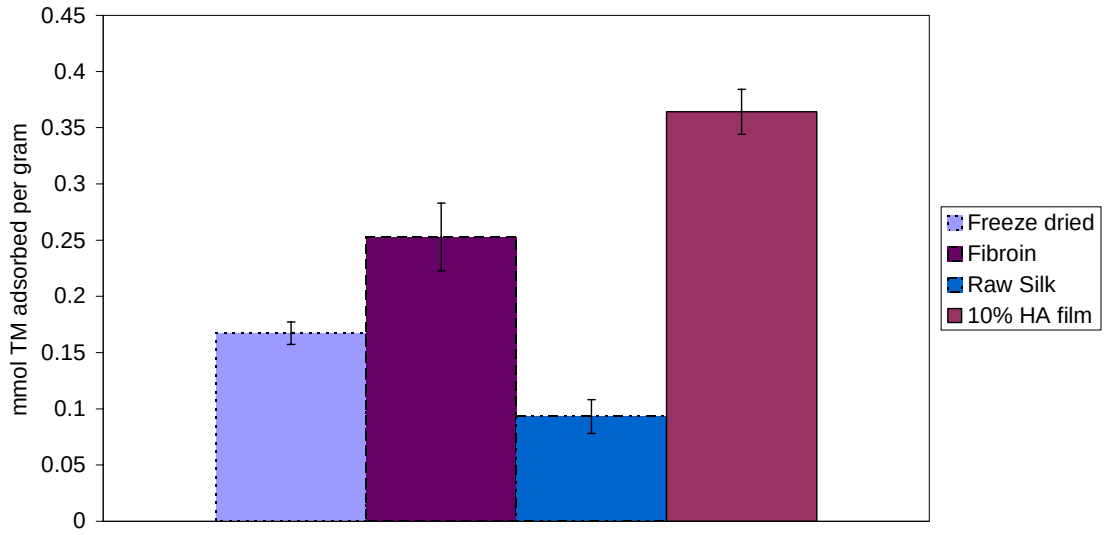

Figure 6.9 Results of adsorption experiment. Equilibrium concentrations.

Adsorption tests were carried out for the two different freeze-dried sponges, raw silk, 10% HA insoluble film, and degummed silk. All the samples adsorbed TM in the first day and released around 20 percent of the adsorbed amount. This is a general trend observed in all the drug uptake experiments. The average adsorbed amount around 0.2-0.35 mmol per gram is depicted in Figure 6.9. This amount was comparable with literature results where commercially available membranes were used [16], which was mentioned in section 2.2.4. It was reported that TM had ionic interaction with carboxyl groups of the methacrylic acid [79]. Same interaction takes place in this study between timolol and carboxylic acid groups of hyaluronic acid. Blending the silk fibroin with 10 % HA has increased drug loading capacity.

6.5. Diffusion Experiments

For the iontophoresis experiments silk fibroin membranes with good mechanical properties were needed. Mechanical strength was required in order to handle the films in the diffusion cell. For this purpose silk fibroin membrane crosslinked by glutaraldehyde were used in the experiments.

6.5.1. Passive Diffusion Experiments

The passive diffusion experiments were performed in the iontophoretic setup with the same buffer solutions and under the same conditions with exception that no current application was present.

6.5.1.1 SFGTA Films

6.5.1.1.1 Drug loaded SFGTA Films

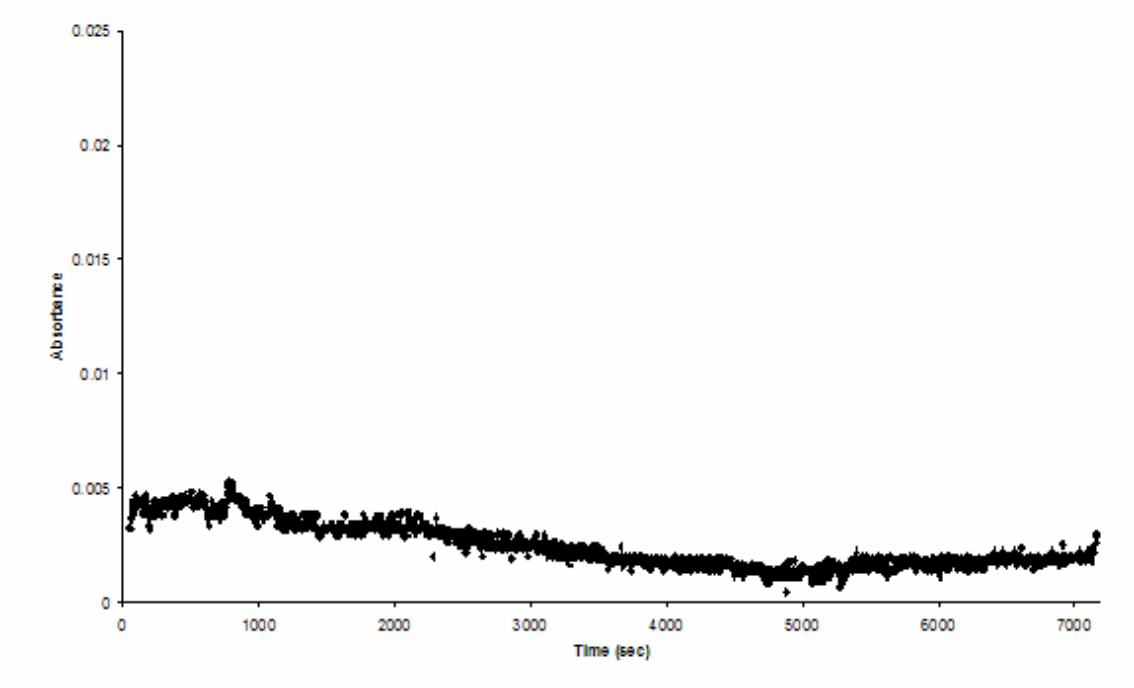

Figure 6.10 Passive drug delivery for SFGTA drug loaded film. I=0.

The passive diffusion results of the drug-loaded with 150 µl eye drop SFGTA membrane showed that the rate of diffusion was related to the concentration gradient. This membrane contained 0.236 millimoles of TM. Flowrate was 4.87 ml/minute. As the drug in the matrix was depleted rate slowed down as depicted in Figure 6.10. It was observed that passive diffusion was unable to mobilize the drug molecules present in the membrane.

6.5.1.1.2 Blank SFGTA Films

When SFGTA membranes were used for passive delivery, they allowed diffusion of very low amounts of drug which was hardly measurable.

6.5.2. Active Diffusion Experiments

In the active diffusion experiments, current was applied to the system after an initial passive diffusion interval of between 20and 30 minutes passed. This passive diffusion interval serves as a basis and is visible in the absorbance results. The current application was performed at three levels: 1, 2, and 4 milliamperes (mA). When divided to the active membrane area of 1.327 cm^2, these currents correspond to current densities of 0.75, 1.5, and 3 mA/ cm^2 respectively. The absorbance results of the active diffusion experiments at three current levels were compared with each other and the passive condition (I=0).

In the following figures, (a) shows the absorption data for the delivery of drug and (b) shows the duration and magnitude of the current applied on the same time scale. Duration of current application is called a "pulse" in this text. The applied dose in the iontophoretic delivery is the current level multiplied with the current application interval. This dose was usually 80 mA minutes, which is the maximum amount deliverable at one run by Iomed power supply. When current was 4 mA, this dose is given in 20 minutes. When current is lowered, duration of current application extends. For instance, when current is reduced by half to 2 mA, duration doubles to 40 minutes.

6.5.2.1 SFGTA Films

6.5.2.1.1 Drug loaded SFGTA Films

Drug loaded with 150 μl eye drop SFGTA membrane was washed with deionized water (DW) for 10 minutes prior to experiment. The thicknesses of the films were 100 μm. Flowrate was 4.5 ml/minute. The membrane contains 0.236 millimoles of TM. There was an initial peak in drug absorption depicted in Figure 6.11. This could be related to the initial washing of the membrane by the buffer flowing down in the receptor compartment. After the gradual reduction in passive diffusion, the first pulse with I=1 mA was given for 40 minutes. Sharp increase and following decrease

was observed in drug release. Then gradual reduction with a similar trend prevailed. The diffusion rate and course were similar with the passive diffusion but when the current was applied, a response was suddenly received. Then the diffusion went back to the same track which was similar to passive diffusion.

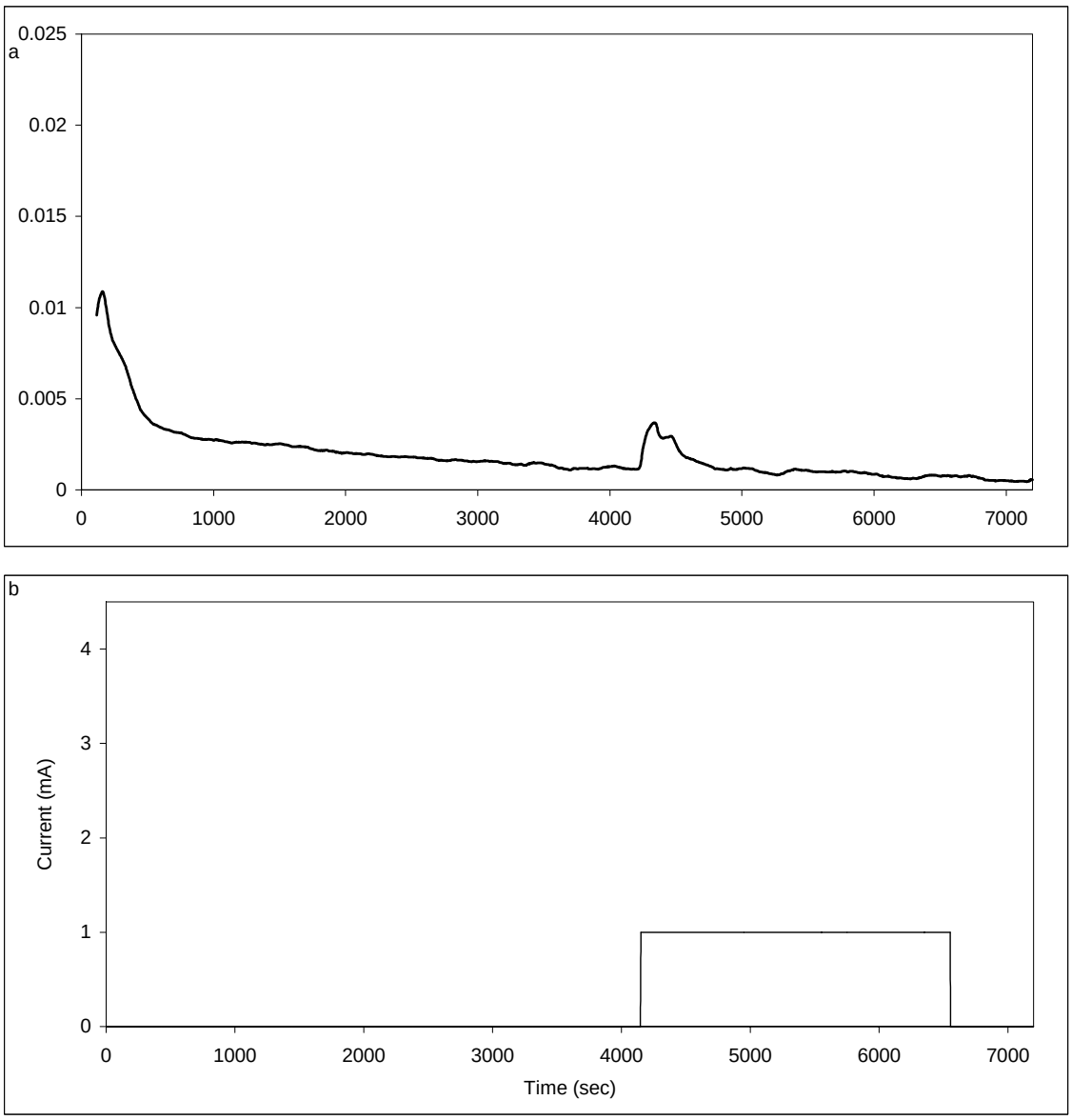

Figure 6.11 a) Iontophoretic drug delivery for SFGTA drug loaded film. b) Current application course with I=1 mA.

It was understood that current application has mobilized some of the drug molecules which were adsorbed or trapped in the membrane. This tells us that the current application has an enhancing effect on transport. However, it was not possible

to control the delivery in an on/off fashion. Another membrane piece was cut from the same film and this time subjected to two different current levels of 2 and 4 mA respectively (Figure 6.12). Flowrate was 4.3 ml/minute. The results of this experiment support the above suggestions. Application of current at 2 mA level produced a quick response of diffusion increase. When another current was applied at the higher value of 4 mA, there was no or very slight response. It is understood that in order to see a prominent increase in diffusion some accumulation of adsorbed or trapped drug molecules should take place. The fact that the magnitude of the response is not closely related to the level of current applied support the suggestion of "enhancing/mobilizing" effect of current. The drug molecules might have been cross-linked by GTA and therefore majority of them may be immobilized. For Figure 6.11 and Figure 6.12, drug release was very low and these figures depict the poor performance of drug loaded membranes. These figures report absorbance data obtained over duration of experiment.

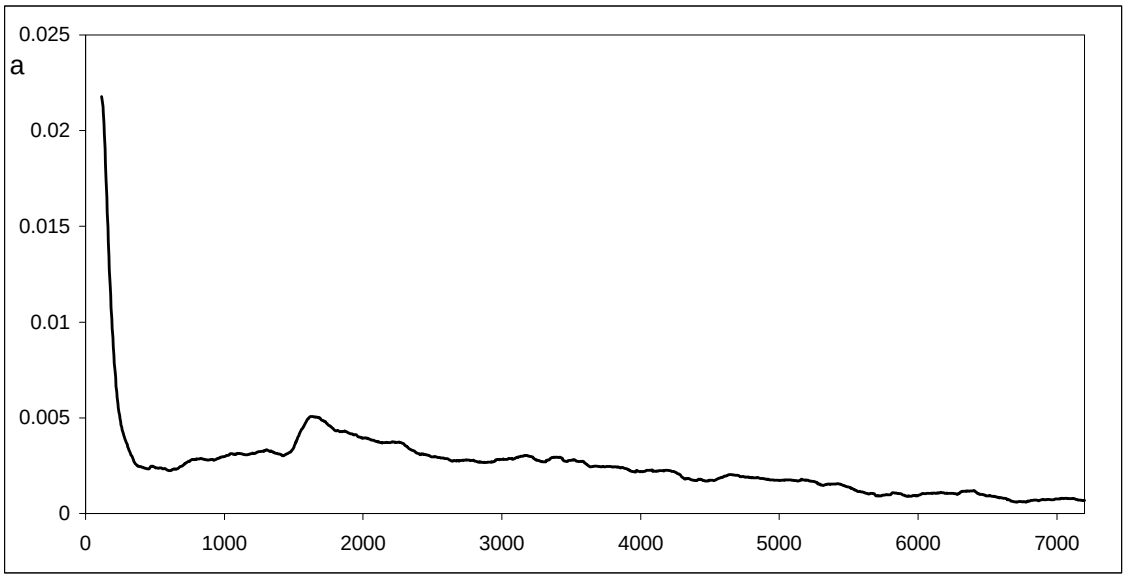

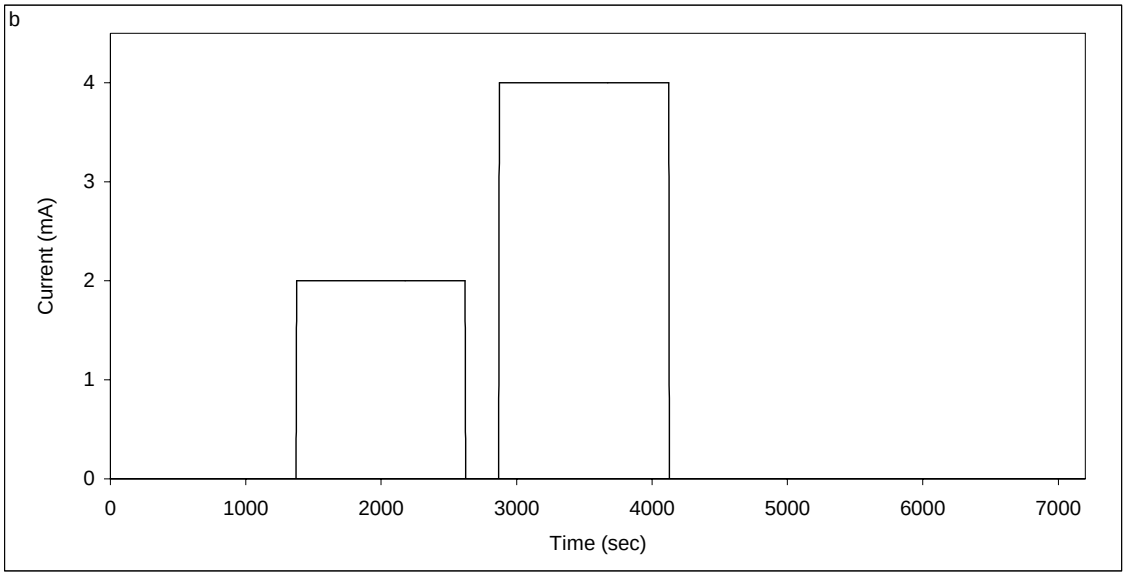

Figure 6.12 a) Iontophoretic drug delivery for SFGTA drug loaded film. b) Current application course of two current applications of I=2 and 4 mA.

Figure 6.12 shows the drug delivery for SFGTA membrane loaded with 150 µl eye drop, having identical properties with membrane whose results were given in Figure 6.11. The membrane contains 0.236 millimoles of TM. It is understood that washing the drug loaded film prior to cutting does not release an amount of drug that will affect diffusion behaviour since this run produced an higher initial peak which indicates that drug in the membrane was not removed by washing.

6.5.2.1.2 Blank SFGTA Films

These films were produced identically with other SFGTA films. The thicknesses of the films are between 90-110 µm. Their behavior under current application and responsiveness has been investigated. Drug loading was 1 ml from the stock solution which contains equivalent drug to the eye drop. This makes 1.572 millimoles of TM. The dose of the delivery was 80 mA minutes for all the three pulsed type experiments. In all the experiments, there was a 20 minutes (1200 sec) of passive initial section.

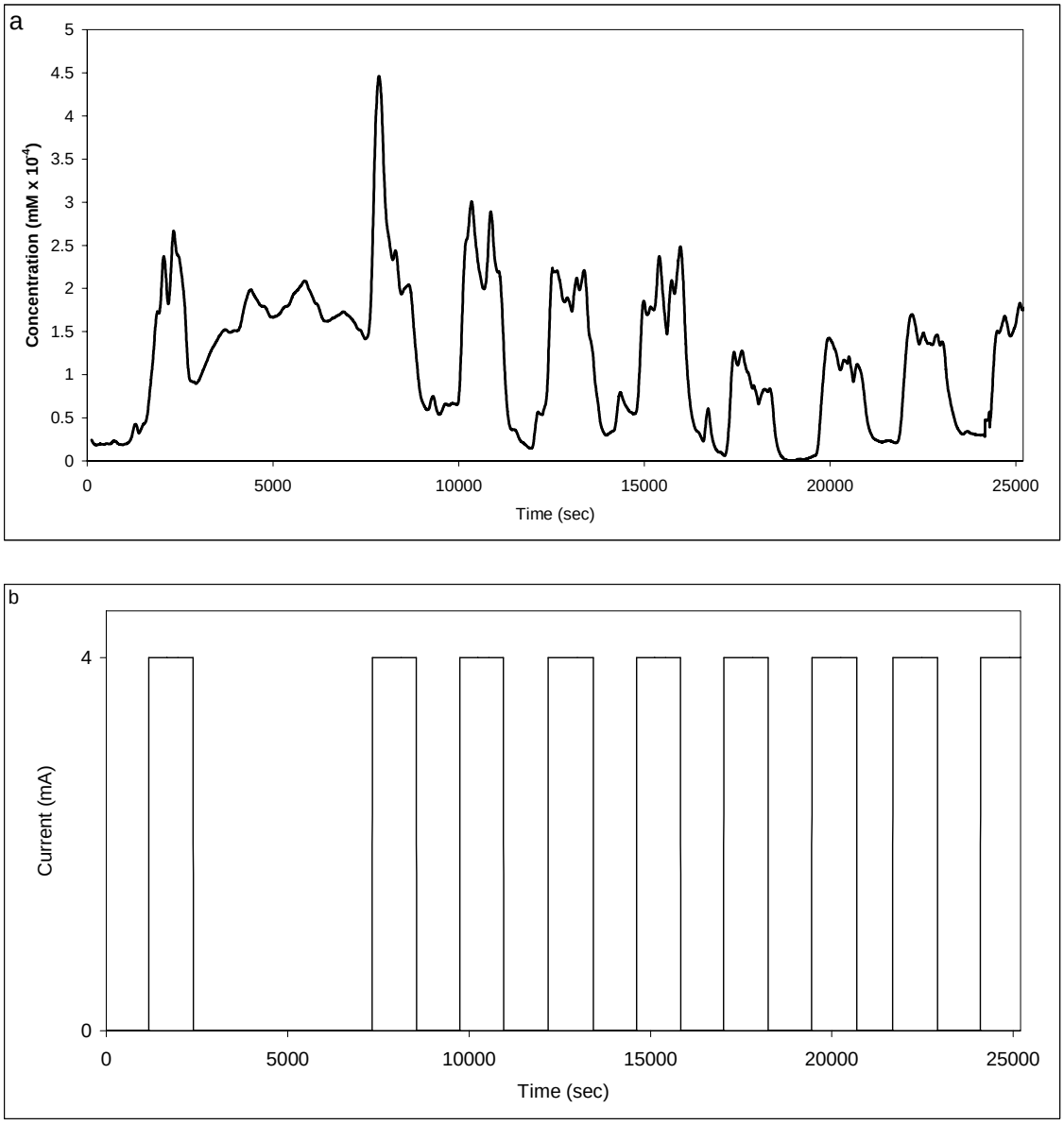

Figure 6.13 Iontophoretic drug delivery experiment for SFGTA membrane. Pulsed current application of I=4 mA a) Delivery of drug b) Current application course.

In Figure 6.13, it is seen that after pulse was given at 4 mA, the released drug concentration showed a sharp increase. Flowrate was 2.83 ml/minute. After pulse ended, delivery level made a steep fall, but not to the initial value. Delivery even increased for sometime and then decreased. Around 80 minutes were given to the system to come to a stable course. Then pulses were given in a regular fashion for 20 minutes and 20 minutes was allowed to pass without current. One cycle was a total of 40 minutes. All of these cycles produce eminent responses in the delivery. As the drug in the receptor compartment was depleted, the peaks get smaller in magnitude and total

area under the curves was similarly reduced. A good control of delivery by current application was achieved.

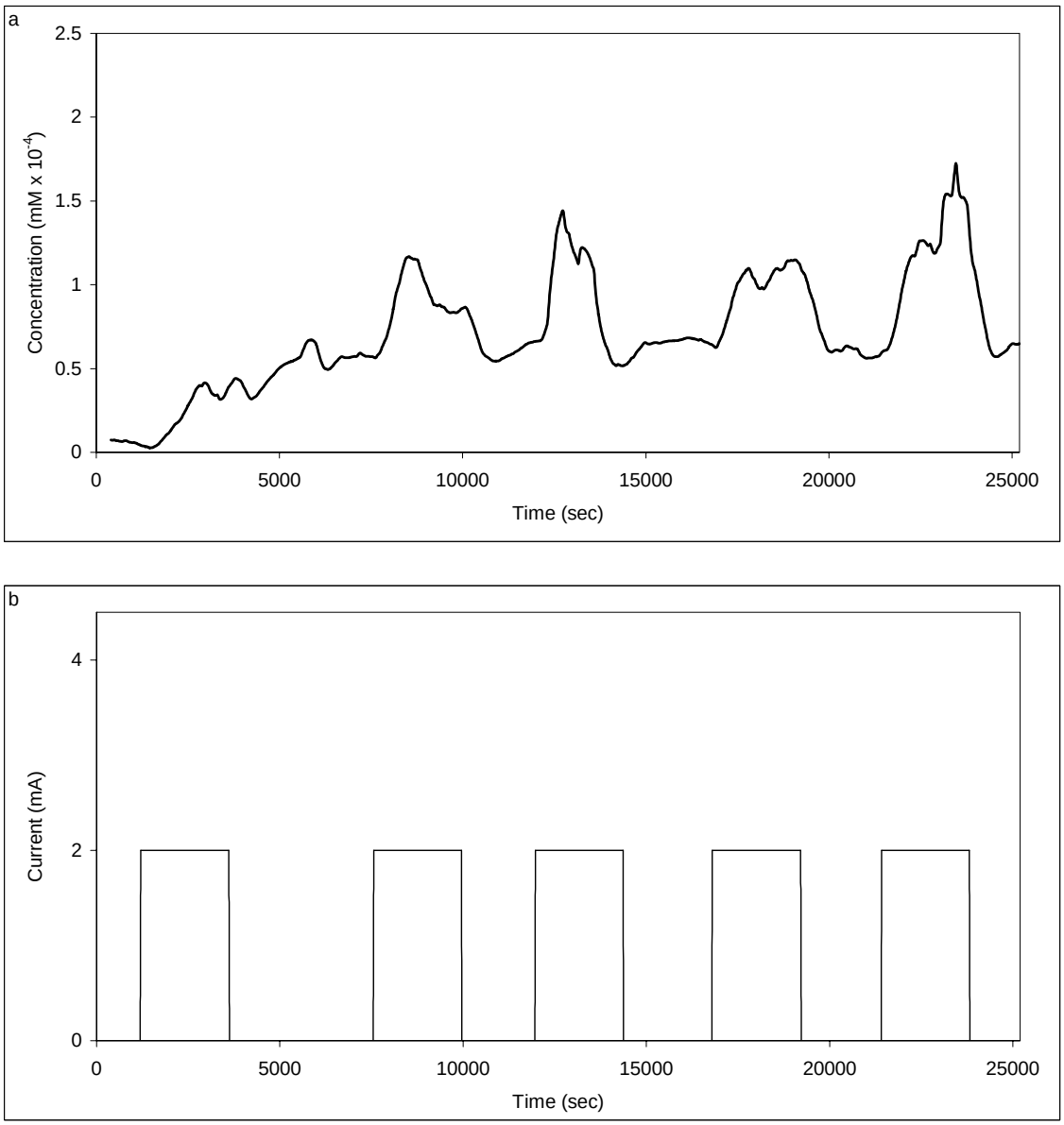

Figure 6.14 Iontophoretic drug delivery experiment for SFGTA membrane. Pulsed current application of I=2 mA a) Delivery of drug b) Current application course.

The amount of released drug for 2 mA pulsed current application was given in Figure 6.14. Flowrate was 3.37 ml/minute. After pulse ends, delivery level continued to increase gradually. After more than one hour, released drug concentration was nearly steady and then pulses were given in a regular fashion for 40 minutes and another 40 minutes was allowed to pass without current, making a cycle of 80 minutes. Again pulses produce visible responses in the delivery. The peaks differed slightly in

magnitude, yet total areas under the curves were approximately same. This is reasonable considering the change in drug concentration in the receptor was slower compared to 4 mA case. Current application could control amount of drug released.

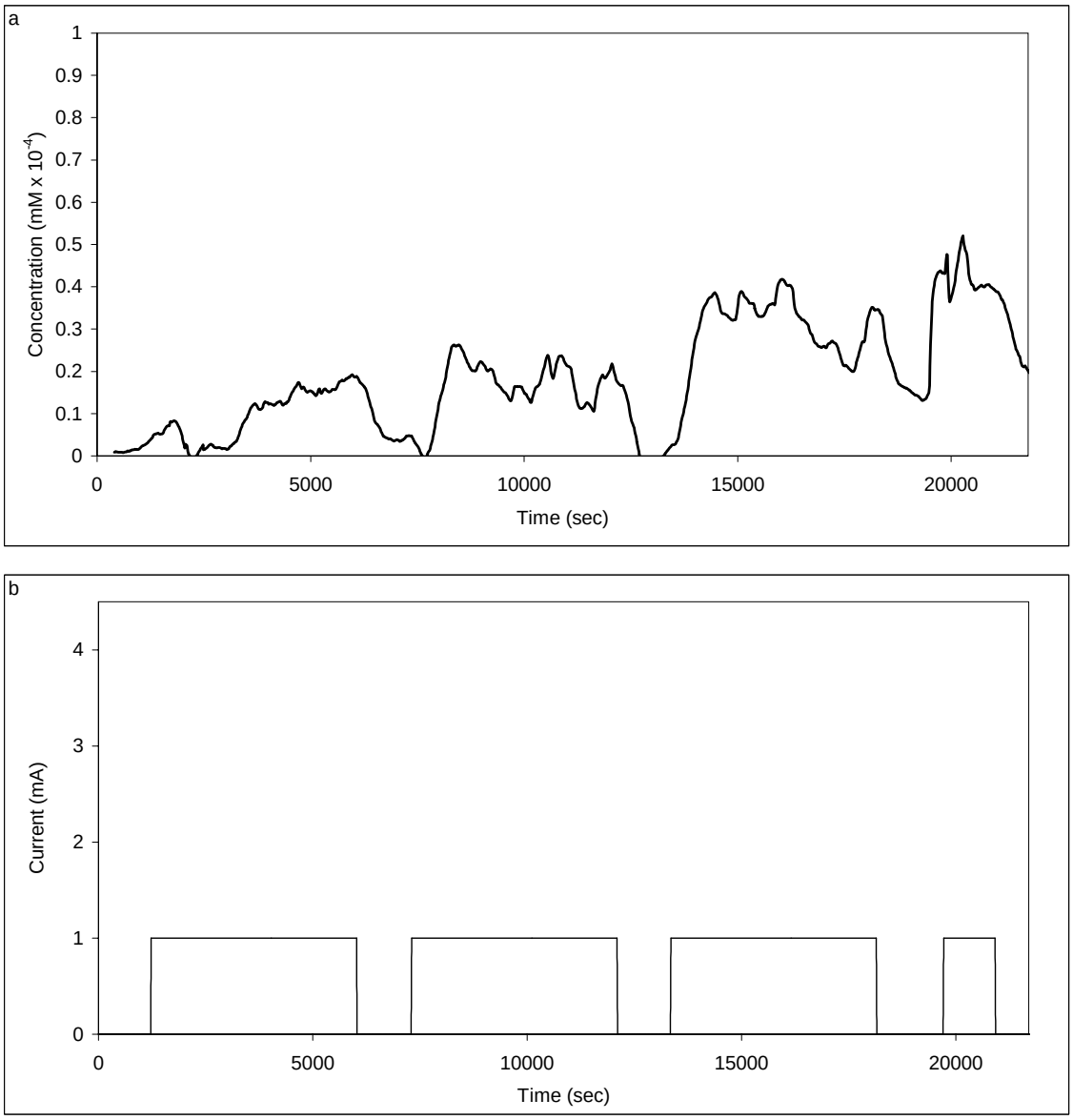

Figure 6.15 Iontophoretic drug delivery experiment for SFGTA membrane. Pulsed current application of I=1 mA a) Delivery of drug b) Current application course.

The result of release experiment with 1 mA pulses is given in Figure 6.15. Flowrate was 3.09 ml/minute. The system gave sluggish response with smaller amplitude compared to 4 and 2 mA cases. There is a 20 minutes interval between the pulses. This time pulses produce responses with increasing magnitude. This is related to the gradual increase in the permeability of the membrane.

Three experiments at 4, 2, and 1 mA current levels are combined in Figure 6.16. It is suggested that there is a threshold value for the permeabilization of the membrane. When current was 4 mA, this threshold value was exceeded after first pulse was given. For 2 mA, threshold value was exceeded after two pulses. Drug depletion does not have a considerable effect on diffusion rate in this case. For the case when current was 1 mA, threshold value was not exceeded during the course of the experiment and there was a gradual process of permeabilization.

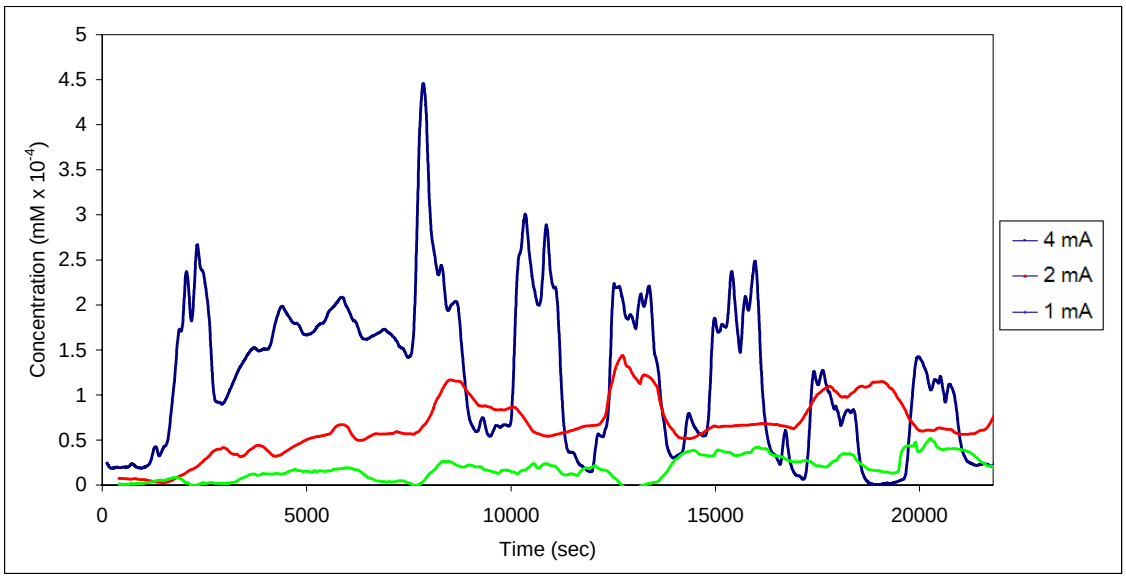

Figure 6.16 Iontophoretic drug delivery for SFGTA membranes pulsed current application values of 1, 2, and 4 mA.

In order to achieve controlled delivery of the drug in a pulsatile manner, current levels of 2 and 4 mA (current densities 1.5 and 3 mA/cm^2) are sufficient. Table 6.3 lists the amount of dosage application for three different current levels. Dosage is obtained by multiplying current and application interval. It was observed that the entire drug injected to the donor compartment passed to the receiver blank buffer solution for the 4 mA case. When current was lowered to 2 mA, 68 % delivery was obtained. Lowering current level further to 1 mA resulted in a low drug release of 3.95 %. 2 mA is the threshold value for permeabilization of the membrane to take place and enable controlled drug release. On the other hand, there is not a quantitative relation between

dosage and delivery. It is understood that current level governs the permeability of the membrane.

Table 6.3 Dose applications and corresponding drug release for iontophoretic experiments

Current level (mA)	Total duration (minute)	Total dose (mA minute)	Drug loading (millimoles)	Drug delivered (millimoles)	Percent delivered	Percent retained
4	180	720	1.47	1.528	103.94	0
2	200	400	1.47	1.000	68	32
1	260	260	1.47	0.058	3.95	96.15

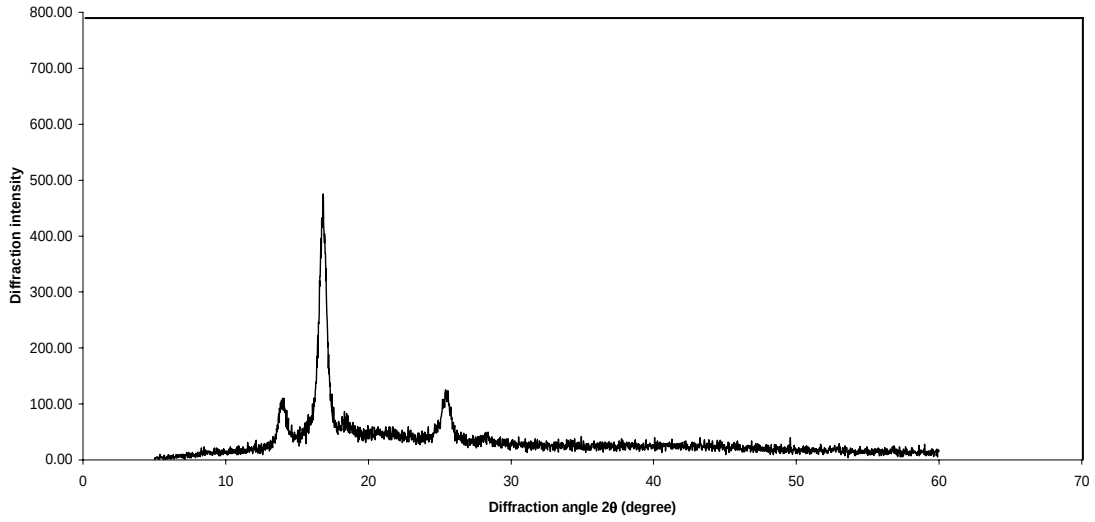

Figure 6.17 X-Ray diffractogram of methanol treated (10 min) SF film after iontophoretic experiment.

The XRD results show that the electric field applied in iontophoretic experiment converts the silk structure to a more crystalline state indicated by an increase in the intensity of peaks. This could be observed when XRD results of methanol treated films

before and after iontophoretic experiments, Figure 6.3 and Figure 6.17 are compared. Electric field application causes an increase of crystallinity in the structure.

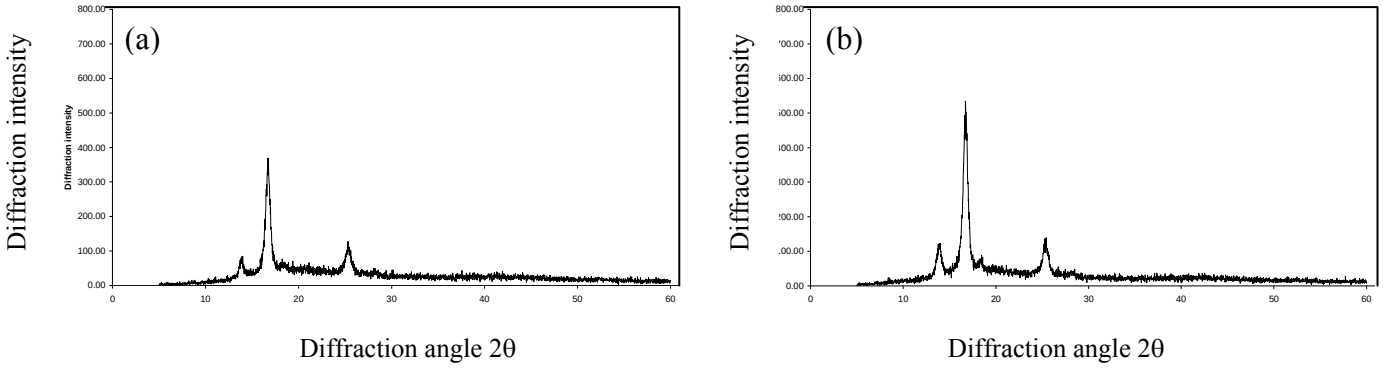

Figure 6.18 X-ray diffractograms of SFGTA film a) Before iontophoresis b) After iontophoresis

XRD patterns in Figure 6.18.a and Figure 6.18.b compares crystallinity of SFGTA film before and after iontophoretic experiment. Electric field favours the protein structure to obtain a more ordered state, which was observed by an increase in crystallinity.

CONCLUSIONS

In this study, various forms of silk fibroin (SF) and SF with blending agents such as hyaluronic acid (HA) have been tested for their feasibility as a potential drug reservoir. These were developed for use in iontophoretic transdermal drug delivery systems. Different forms of silk and silk fibroin, such as raw silk, degummed SF, insolubilized freeze-dried SF, SF blended with HA were investigated for their adsorption capacity of timolol, which was used as the model drug. The observed drug uptake capacities were close to those of commercial membranes in the market. Fibroin, freeze-dried SF, and SF/HA films were compared to raw silk for drug loading capacity. Insolubilization of membranes by post treatment, manipulation of drying conditions, and blending with different agents were successfully achieved. Configurational changes of fibroin protein and interactions between SF and HA were investigated by Ft-Ir and XRD analyses. The obtained insoluble membranes were investigated for drug delivery performance in a custom-made diffusion cell under passive diffusion and iontophoretic conditions. It was demonstrated that the silk fibroin glutaraldehyde and methanol treated fibroin films could be successfully used for controlled drug delivery. There is a threshold value for permeabilization of the membrane. It was found that current densities 1.5 and 3 mA/cm^2 were suitable to accomplish controlled delivery of the drug in a pulsatile manner. The results of this study should be useful in controlled transdermal delivery of positively charged drug molecules.

REFERENCES

1 A.E. Vasil'ev, I.I. Krasnyuk, S. Ravikumar, V.N. Tokmakhchi, Drug synthesis methods and manufacturing technology, Transdermal Therapeutic Systems For Controlled Drug Release (A Review), Pharmaceutical Chemistry Journal, Vol. 35, No. 11, 2001

2 Fletcher K., Drug delivery: strategies and technologies, PSTT Vol. 1, No. 2, 1998

3 Yogeshvar N. Kalia , Aarti Naik , James Garrison, Richard H. Guy, Modeling transdermal drug release, Advanced Drug Delivery Reviews 48 (2001) 159–172

4 Mingzhong Li, Shenzhou Lu, Zhengyu Wu, Ke Tan, Norihiko Minoura, Shigenori Kuga, Structure and properties of silk fibroin–poly(vinyl alcohol) gel, International Journal of Biological Macromolecules, 30, 2002

5 Yu-Qing Zhang, Biotechnology Advances, Natural silk fibroin as a support for enzyme immobilization, vol. 16, Nos. 5/6, 961–971, 1998

6 In Chul Um, HaeYong Kweon, Young Hwan Park, Sam Hudson, Structural characteristics and properties of the regenerated silk fibroin prepared from formic acid, International Journal of Biological Macromolecules, 29 (2001) 91–97

7 Jaskari T., Vuorio M., Urtti A., Manzanares J. A., Hirvonen J., Controlled transdermal iontophoresis by ion-exchange fiber, Journal of Controlled Release, 67 (2000) 179–190

8 Ebtessam A. Essa, Michael C. Bonner, Brian W. Barry, Iontophoretic estradiol skin delivery and tritium exchange in ultradeformable liposomes, International Journal of Pharmaceutics 240 (2002) 55–66

9 Yogeshvar N. Kalia , Richard H. Guy, Modeling transdermal drug release, Advanced Drug Delivery Reviews 48 (2001) 159–172

10 Banga A. K., Chien Y. W., Hydrogel Based Iontotherapeutic Delivery Devices for Transdermal Delivery of Peptide/Protein Drugs, Pharmaceutical Research, Vol. 10, No. 5, 1993

11 Barry B. W., Is transdermal drug delivery research still important today?, DDT (Drug delivery tech.), Vol. 6, No. 19, 2001

12 Banga A. K., Transdermal Iontophoretic Drug Delivery, Drug Delivery

13 Banga A.K., Prausnitz M.R., Tibtech, Assessing the potential of skin electroporation for the delivery of protein- and gene-based drugs, Vol. 16, October 1998

14 Anthony F. Coston, John K.-J. Li, Iontophoresis: Modeling, Methodology, and Evaluation, Cardiovascular Engineering: An International Journal, Vol. 1, No. 3, September 2001

15 Richard H. Guy , Yogeshvar N. Kalia , M. Begona Delgado-Charro, Virginia Merino , Alicia Lopez , Diego Marro, Iontophoresis: electrorepulsion and electroosmosis, Journal of Controlled Release 64 (2000) 129–132

16 Ruey-Yih Lin, Yih-Chien Ou, Wen-Yih Chen, The role of electroosmotic flow on in-vitro transdermal iontophoresis, Journal of Controlled Release 43 (1997) 23–33

17 D.F. Stamatialis, H.H.M. Rolevink, G.H. Koops, Controlled transport of timolol maleate through artificial membranes under passive and iontophoretic conditions, Journal of Controlled Release, 81 (2002) 335–345

18 Jaskari T., Vuorio M., Kontturi K., Manzanares J. A., Hirvonen J., Ion-exchange fibers and drugs: an equilibrium study, Journal of Controlled Release, 70 (2001) 219–229

19 Tarvainen T., Svarfvar B., Akerman S., Savolainen J., Karhu M., Paronen P., Jarvinen K., Drug release from a porous ion-exchange membrane *in vitro*, Biomaterials, 20 (1999) 2177–2183

20 Akerman S., Viinikka P., Svarfvar B., Jarvinen K., Nasman J., Urtti A., Paronen P., Transport of drugs across porous ion exchange membranes, Journal of Controlled Release, 50 (1998) 158–166

21 Akerman S., Svarfvar B., Kontturi K., Nasman J., Urtti A., Paronen P., Jarvinen K., Influence of ionic strength on drug adsorption onto and release from a poly(acrylic acid) grafted poly(vinylidene fluoride) membrane, International Journal of Pharmaceuticals, 178 (1999) 67–75

22 Kankkunen T., Sulkava R., Vuorio M., Kontturi K., Hirvonen J., Transdermal iontophoresis of tacrine *in vivo*, Pharmaceutical Research, Vol. 19, No. 5, 2002

23 Tarja Kankkunen , Inkeri Huupponen , Katri Lahtinen , Mats Sundell , Kenneth Ekman , Kyosti Kontturi , Jouni Hirvonen, Improved stability and release control of levodopa and metaraminol using ion-exchange fibers and transdermal iontophoresis, European Journal of Pharmaceutical Sciences 16 (2002) 273–280

24 Jouni Hirvonen , Lasse Murtomaki , Kyosti Kontturi, Experimental verification of the mechanistic model for transdermal transport including iontophoresis, Journal of Controlled Release 56 (1998) 169–174

25 D.Voet, J.G.Voet, Biochemistry, New York: John Wiley and Sons, c1995

26 Hirai Y., Ishikuro J., Nakajima T., Some comments on the penetration of water vapour into regenerated silk fibroin, Polymer 42 (2001) 5495–5499

27 Yu-Qing Zhang, Applications of natural silk protein sericin in biomaterials, Biotechnology Advances, 20 (2002) 91–100

28 Yamada H., Nakao H., Takasu Y., Tsubouchi K., Preparation of undegraded native molecular fibroin solution from silkworm cocoons, Materials Science and Engineering C 14 (2001) 41–46

29 Mukhamedzhanova M. Yu., Takhtaganova D.B., Pak T.S., Properties of concentrated solutions of fibroin and its derivatives, Chemistry of Natural Compounds, Vol. 37, No. 4, 2001

30 Mingzhong Li, Masayo Ogiso, Norihiko Minoura, Enzymatic degradation behavior of porous silk fibroin sheets, Biomaterials 24 (2003) 357–365

31 G. Freddi, G. Pessina, M. Tsukada, Swelling and dissolution of silk fibroin (*Bombyx mori*) in *N*-methyl morpholine *N*-oxide, International Journal of Biological Macromolecules 24 (1999) 251–263

32 Lim V. I., Steinberg S. V., A novel structural model for silk fibroin: $\alpha_L\alpha_R\beta$-structure, FEBS Letters, Vol. 131 No. 2, pp. 203–207, 1981

33 Xin Chen, Zhengzhong Shao, Nebojsa S. Marinkovic, Lisa M. Miller, Ping Zhou, Mark R. Chance, Conformation transition kinetics of regenerated *Bombyx mori* silk fibroin membrane monitored by time-resolved Ft-ir spectroscopy, Biophysical Chemistry 89 2001 25–34

34 Altman G, H., Diaz F., Jakuba C., Calabro T., Horan R. L., Chen J., Lu H., Richmond J., Kaplan D. L., Silk-based biomaterials, Biomaterials 24 (2003) 401–416

35 Balköse D., Doğal ve değiştirilmiş ipek fibroininin kimi fizikokimyasal özelliklerinin incelenmesi (Doçentlik tezi), Ege Üniversitesi, 1982

36 T. Furuzono, K. Ishihara, N. Nakabayashi, Y. Tamada, Chemical modification of silk fibroin with 2-methacryloyloxyethyl phosphorylcholine. II. Graft-polymerization onto fabric through 2-methacryloyloxyethyl isocyanate and interaction between fabric and platelets, Biomaterials 21 (2000) 327–333

37 Jun Magoshi, Yoshiko Magoshi, Mary A. Becker, Masao Kato, Zhang Han, Toshihisa Tanaka, Shun-ichi Inoue, Shigeo Nakamura, Crystallization of silk Fibroin from solution, *Thermochimica Acta* 352–353 (2000) 165–169

38 Gregory H. Altman, Rebecca L. Horan, Helen H. Lu, Jodie Moreau, Ivan Martin, John C. Richmond, David L. Kaplan, Silk matrix for tissue engineered anterior cruciate ligaments, Biomaterials 23 (2002) 4131–4141

39 Kweon H.Y., Park S.H., Yeo J.H., Cho C.S., Preparation of semi-interpenetrating polymer networks composed of silk fibroin and poly(ethylene glycol) macromer, Journal of Applied Polymer Science, Vol. 80, 1848–1853 (2001)

40 Putthanarat S., Zarkoob S., Magoshi J., Chen J.A., Eby R.K., Stone M., Adams W.W., Effect of processing temperature on the morphology of silk membranes, Polymer 43 (2002) 3405–3413

41 Kazunori Tanaka, Naoki Kajiyama, Kiyohide Ishikura, Shou Waga, Aiko Kikuchi, Kohei Ohtomo, Takashi Takagi, Shigeki Mizuno, Determination of the site of disulfide linkage between heavy and light chains of silk fibroin produced by *Bombyx mori*, *Biochimica et Biophysica Acta* 1432 (1999) 92–103

42 Xiao Zheng Shu, Yanchun Liu, Fabio Palumbo, Glenn D. Prestwich, Disulfide-crosslinked hyaluronan-gelatin hydrogel films: a covalent mimic of the extracellular matrix for *in vitro* cell growth, Biomaterials 24 (2003) 3825–3834

43 Seves A., Romano M., Maifreni T., Sora S., Ciferri O., The microbial degradation of silk: a laboratory investigation, International Biodeterioration & Biodegradation 42 (1998) 203–211

44 R. Nemoto, S. Nakamura, T. Isobe, M. Senna, Direct Synthesis of Hydroxyapatite-Silk Fibroin Nano-Composite Sol via a Mechanochemical Route, Journal of Sol-Gel Science and Technology, 21, 7–12, 2001

45 Minoura N., Tsukada M., Nagura M., Fine structure and oxygen permeability of silk fibroin membrane treated with methanol, Polymer, 1990, Vol. 31, February

46 Editor-in-Chief: Salamone J. C., Polymeric Materials Encyclopedia, CRC Press, New York, 1996

47 Minoura N., Tsukada M., Nagura M., Physico-chemical properties of silk fibroin membrane as a biomaterial, Biomaterials 1990, Vol. 11 August

48 Liu H., Zhang Z., Zhang X., Qi D., Liu Y., Yu T., Deng J., A phenazine methosulphate-mediated sensor sensitive to lactate based on entrapment of lactate oxidase and horseradish peroxidase in composite membranes of poly(vinyl alcohol) and regenerated silk fibroin, *Electrochimica Acta*, Vol. 42, No. 3, pp. 349–355, 1997

49 Cheng Qiong, Peng Tuzhi, Yang Liju, Silk Fibroin/cellulose acetate membrane electrodes incorporating xanthine oxidase for the determination of Fish freshness, *Analytica Chimica Acta*, 369, 1998

50 Liu H., Deng H., Sun K., Qi D., Deng J., Liu Y., Yu T., Structure and properties of regenerated silk fibroin and poly(vinyl alcohol) and biosensing of glucose via Meldola blue dispersed in polyester ionomer as an electron transfer mediator, Fresenius Journal of Analytical Chemistry, (1997) 357: 812–816

51 Gotoh Y., Tsukada M., Baba T., Minoura N., Physical properties and structure of poly(ethylene glycol)-silk fibroin conjugate films, Polymer, Vol. 38 No. 2, pp. 487–490, 1997
52 Tsukada M., Freddi G., Minoura N., Allara G., Preparation and application of porous silk fibroin materials, Journal of Applied Polymer Science, Vol. 54, 507–514, 1994
53 Eliana Leo, Maria Angela Vandelli, Riccardo Cameroni, Flavio Forni, Doxorubicin-loaded gelatin nanoparticles stabilized by glutaraldehyde: Involvement of the drug in the cross-linking process, International Journal of Pharmaceutics 155 (1997) 75–82
54 Raymond Zeeman, Pieter J. Dijkstra, Pauline B. van Wachem, Marja J.A. van Luyn, Marc Hendriks, Patrick T. Cahalan, Jan Feijen, Successive epoxy and carbodiimide cross-linking of dermal sheep collagen, Biomaterials 20 (1999) 921–931
55 Jianyong C., Tanioka A., Minoura N., Sen-I Gakkaishi, Membrane potential of weak amphoteric polymer membrane composed of silk fibroin, Vol. 49, No. 9, 1993
56 Jianyong C., Tanioka A., Minoura N., Sen-I Gakkaishi, Ion permeabilities across silk fibroin membrane, Vol. 50, No. 1, 1994
57 Chen J., Minoura N., Osaki T., Tanioka A., Effects of pH on the transport of 5-fluorouracil across a fibroin membrane, Transaction, Vol. 56, No. 6, 2000
58 Chen J., Minoura N., Tanioka A., Transport of pharmaceuticals through silk fibroin membrane, Polymer, Vol. 35, No. 13, pp. 2853–2856, 1994
59 T. Koyano, N. Koshizaki, H. Umehara, M. Nagura, N. Minoura, Surface states of PVA/chitosan blended hydrogels, Polymer 41 (2000) 4461–4465
60 K.Y. Cho, T.W. Chung, B.C. Kim, M.K. Kim, J.H. Lee, W.R. Wee, C.S. Cho Release of ciprofloxacin from poloxamer-graft-hyaluronic acid hydrogels *in vitro*, International Journal of Pharmaceutics 260 (2003) 83–91
61 Yi Luo , Kelly R. Kirker , Glenn D. Prestwich, Cross-linked hyaluronic acid hydrogel films: new biomaterials for drug delivery, Journal of Controlled Release 69 (2000) 169–184
62 Francesca Maccari, Francesca Tripodi, Nicola Volpi, High-performance capillary electrophoresis separation of hyaluronan oligosaccharides produced by Streptomyces hyalurolyticus hyaluronate lyase, Carbohydrate Polymers (2004)
63 Michael Jahn, John W. Baynes, Gerhard Spiteller, The reaction of hyaluronic acid and its monomers, glucuronic acid and *N*-acetylglucosamine, with reactive oxygen species, Carbohydrate Research 321 (1999) 228–234
64 Seon Jeong Kim , Chang Kee Lee , Young Moo Lee , In Young Kim , Sun I. Kim, Electrical / pH-sensitive swelling behavior of polyelectrolyte hydrogels prepared with hyaluronic acid–poly(vinyl alcohol) interpenetrating polymer networks, Reactive & Functional Polymers 55 (2003) 291–298
65 Seon Jeong Kim, Seoung Gil Yoon, Young Moo Lee, Hee Chan Kim, Sun I. Kim, Electrical behavior of polymer hydrogel composed of poly(vinyl alcohol)–hyaluronic acid in solution, Biosensors and Bioelectronics 19 (2004) 531–536
66 Deriu A., Cavatorta F., Micheli T. D., Rupprecht A., Langan P., The distribution of water in highly ordered fibres of hyaluronic acid, *Physica* B 234–236 (1997) 215–216
67 Jamal Alyoussef Alkrad, Yahya Mrestani, Dieter Stroehl, Siegfried Wartewig, Reinhard Neubert, Characterization of enzymatically digested hyaluronic acid

using NMR, Raman, IR, and UV–Vis spectroscopies, Journal of Pharmaceutical and Biomedical Analysis 31 (2003) 545–550

68 Yong Doo Park, Nicola Tirelli, Jeffrey A. Hubbell, Photopolymerized hyaluronic acid-based hydrogels and interpenetrating networks, Biomaterials 24 (2003) 893–900

69 Park S.N., Park J.C., Kim H.O., Song M. J., Suh H., Characterization of porous collagen/hyaluronic acid scaffold modified by 1-ethyl-3-(3-dimethylaminopropyl)carbodiimide cross-linking, Biomaterials, 23 (2002) 1205–1212

70 Glenn D. Prestwich , Dale M. Marecak , James F. Marecek , Koen P. Vercruysse , Michael R. Ziebell, Controlled chemical modification of hyaluronic acid: synthesis, applications, and biodegradation of hydrazide derivatives, Journal of Controlled Release 53 (1998) 93–103

71 Mee Ryang Kim, Tae Gwan Park, Temperature-responsive and degradable hyaluronic acid / Pluronic composite hydrogels for controlled release of human growth hormone, Journal of Controlled Release 80 (2002) 69–77

72 Si-Nae Park, Hye Jung Lee, Kwang Hoon Lee, Hwal Suh, Biological characterization of EDC-crosslinked collagen–hyaluronic acid matrix in dermal tissue restoration, Biomaterials 24 (2003) 1631–1641

73 G. D. Prestwich, K. P. Vercruysse, Therapeutic applications of hyaluronic acid and hyaluronan derivatives, PSST Vol. 1, No. 1, 1998

74 S.T. Lim , G.P. Martin , D.J. Berry , M.B. Brown, Preparation and evaluation of the *in vitro* drug release properties and mucoadhesion of novel microspheres of hyaluronic acid and chitosan, Journal of Controlled Release, 66 (2000) 281–292

75 Simon L.D., Stella V.J., Charman W.N., Charman S.A., Mechanisms controlling diffusion and release of model proteins through and from partially esterified hyaluronic acid membranes, Journal of Controlled Release 61 (1999) 267–279

76 Simon L.D., Charman W.N., Charman S.A., Stella V.J., Protein transport across hydrated hyaluronic acid ester membranes: Evaluation of ribonuclease A as a potentially useful model protein, Journal of Controlled Release 45 (1997) 273–285

77 S. Barbault-Foucher , R. Gref , P. Russo , J. Guechot , A. Bochot, Design of poly-ε-caprolactone nanospheres coated with bioadhesive hyaluronic acid for ocular delivery, Journal of Controlled Release 83 (2002) 365–375

78 Mi F. L., Sung H. W., Shyu S. S., Drug release from chitosan-alginate complex beads reinforced by a naturally occurring cross-linking agent, Carbohydrate Polymers 48 (2002) 61–72

79 N. Kanikkannan, J. Singh, P. Ramarao, *In vitro* transdermal iontophoretic transport of timolol maleate: effect of age and species, Journal of Controlled Release 71 (2001) 99–105

80 Riitta Sutinen , Petteri Paronen, Arto Urtti, Water-activated, pH-controlled patch in transdermal administration of timolol I. Preclinical tests, European Journal of Pharmaceutical Sciences 11 (2000) 19–24

81 H. Hiratani, C. Alvarez-Lorenzo, Timolol uptake and release by imprinted soft contact lenses made of *N,N*-diethylacrylamide and methacrylic acid, Journal of Controlled Release 83 (2002) 223–230

82 Tsujino M., Isobe T., Senna M., Preparation of silica-silk fibroin-polyurethane composite films via a sol-gel route, Journal f Sol-Gel Science and Technology 19, 785–789, 2000

83 Venter J. P., Müller, A comparative study of an *in situ* adapted diffusion cell and an *in vitro* Franz diffusion cell method for transdermal absorption of doxylamine

84 In Chul Um, HaeYong Kweon, Kwang Gill Lee, Young Hwan Park, The role of formic acid in solution and crystallization of silk protein polymer, International Journal of Biological Macromolecules, 33 (2003) 203–213

85 Tsuboi Y., Ikejiri T., Shiga S., Yamada K., Itaya A., Light can transform the secondary structure of silk protein (rapid communication), Applied Physics A 73, 637–640, 2001

86 S.L. Turgeon , M. Beaulieu , C. Schmitt , C. Sanchez, Protein–polysaccharide interactions: phase-ordering kinetics, thermodynamic and structural aspects, Current Opinion in Colloid and Interface Science 8 (2003) 401–414

87 Sang-Gyun Kim, Gyun-Taek Lim, Jonggeon Jegal, Kew-Ho Lee, Pervaporation separation of MTBE (methyl tert-butyl ether) and methanol mixtures through polyion complex composite membranes consisting of sodium alginate/chitosan, Journal of Membrane Science 174 (2000) 1–15

APPENDIX A

Correlation between Timolol Maleate Concentration and UV Absorbance

UV Analysis: Full spectrum analysis was performed for TM solution and it was observed TM had yielded absorption at 294 nm wavelength. A calibration curve for analysis of TM at UV spectrophotometer (Shimadzu UV-1601) was obtained by analyzing known concentrations of TM at a wavelength of 294 nm.

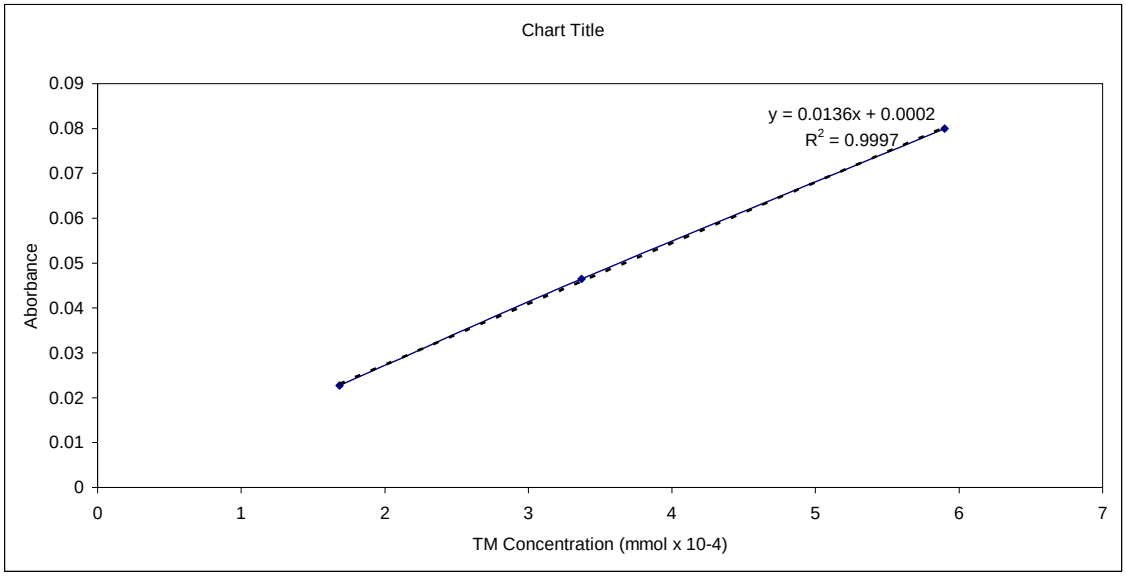

Figure A1. Calibration curve for TM concentration at 294 nm

APPENDIX B

Formulas of Amino acids in Silk Fibroin

The most abundant amino acids found in silk fibroin chain are given below.

Glycine

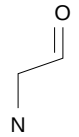

Alanine

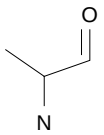

Serine

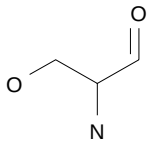

With amino groups:

Lysine

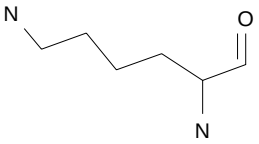

Arginine

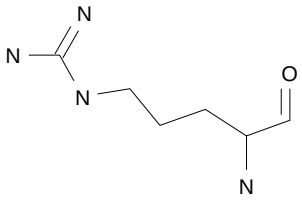

With a thiol group (containing sulphur):

Cysteine

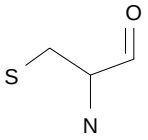

APPENDIX C

Structure of Alpha Helix

In the α helix, every fourth AA forms an H-bond between a carbonyl- and an imino group. Side chains point away from the helix.

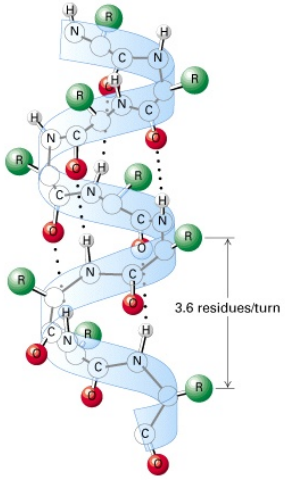

APPENDIX D

Smoothing by MathCAD

Smoothing of data was performed using MathCAD 7 Professional by median smoothing method. This method returns an m-element vector created by smoothing vy with running medians. Span value is set to 7.